Received: 21 March 2021 | Revised: 17 February 2022 | Accepted: 21 March 2022

DOI: 10.1002/ar.24949

SPECIAL ISSUE ARTICLE

The Anatomical Record

WILEY

Anatomy and relationships of the early diverging Crocodylomorphs *Junggarsuchus sloani* and *Dibothrosuchus elaphros*

Alexander A. Ruebenstahl[1,2] | **Michael D. Klein**[3] | **Hongyu Yi**[4,5] | **Xing Xu**[4,5] | **James M. Clark**[1]

[1]Department of Biological Sciences, George Washington University, Washington, District of Columbia, USA

[2]Department of Earth and Planetary Sciences, Yale University, New Haven, Connecticut, USA

[3]Tucson, Arizona, USA

[4]Key Laboratory for the Evolutionary Systematics of Vertebrates of the Chinese Academy of Sciences, Institute of Vertebrate Paleontology and Paleoanthropology, Beijing, China

[5]CAS Center of Excellence in Life and Paleoenvironment, Beijing, China

Correspondence
Alexander A. Ruebenstahl, Department of Earth and Planetary Sciences, Yale University, P.O. Box 208109, New Haven, CT 06520-8109, USA.
Email: alex.ruebenstahl@yale.edu

Funding information
Data Center of Management Science, National Natural Science Foundation of China - Peking University, Grant/Award Number: 41688103; National Science Foundation, Grant/Award Number: EAR 1636753

Abstract

The holotype of *Junggarsuchus sloani*, from the Shishugou Formation (early Late Jurassic) of Xinjiang, China, consists of a nearly complete skull and the anterior half of an articulated skeleton, including the pectoral girdles, nearly complete forelimbs, vertebral column, and ribs. Here, we describe its anatomy and compare it to other early diverging crocodylomorphs, based in part on CT scans of its skull and that of *Dibothrosuchus elaphros* from the Early Jurassic of China. *Junggarsuchus* shares many features with a cursorial assemblage of crocodylomorphs, informally known as "sphenosuchians," whose relationships are poorly understood. However, it also displays several derived crocodyliform features that are not found among most "sphenosuchians." Our phylogenetic analysis corroborates the hypothesis that *Junggarsuchus* is closer to Crocodyliformes, including living crocodylians, than are *Dibothrosuchus* and *Sphenosuchus*, but not as close to crocodyliforms as *Almadasuchus* and *Macelognathus*, and that the "Sphenosuchia" are a paraphyletic assemblage. *D. elaphros* and *Sphenosuchus acutus* are hypothesized to be more closely related to Crocodyliformes than are the remaining non-crocodyliform crocodylomorphs, which form several smaller groups but are largely unresolved.

KEYWORDS

Crocodylomorpha, CT scanning, Jurassic, phylogeny

1 | INTRODUCTION

The "Sphenosuchia" (Bonaparte, 1971, 1984) are archosaurs known from the Late Triassic to the Late Jurassic (Clark et al., 2001; Göhlich et al., 2005; Leardi et al., 2017) that fall within Crocodylomorpha (Hay, 1930) but outside Crocodyliformes. Crocodyliformes includes living crocodylian species and their extinct relatives that possess specializations that solidify the skull (Benton & Clark, 1988; Langston, 1973; Pol et al., 2013) and Crocodylomorpha is the most inclusive clade containing *Crocodylus niloticus* (Laurenti, 1768), but not *Rauisuchus tiradentes* (Huene, 1942), *Poposaurus gracilis* (Mehl, 1915), *Gracilisuchus stipanicicorum* (Romer, 1972),

Prestosuchus chiniquensis (Huene, 1942), or *Aetosaurus ferratus* (Fraas, 1877; Irmis et al., 2013). At least 13 valid monotypic genera are considered potential "sphenosuchians" (referred to as non-crocodyliform crocodylomorphs below): *Sphenosuchus acutus* (Haughton, 1915; Walker, 1990), *Saltoposuchus connectens* (Huene, 1921; Sereno & Wild, 1992), *Hallopus victor* (Marsh, 1877; Walker, 1970), *Terrestrisuchus gracilis* (Crush, 1984), *Dibothrosuchus elaphros* (Simmons, 1965; Wu & Chatterjee, 1993), *Hesperosuchus agilis* (Colbert, 1952), *Pseudhesperosuchus jachaleri* (Bonaparte, 1971), *Litargosuchus leptorhynchus* (Clark & Sues, 2002; *Kayentasuchus walkeri* (Clark & Sues, 2002), *Dromicosuchus grallator* (Sues et al., 2003), *Macelognathus vagans* (Göhlich et al., 2005; Marsh, 1884), *Almadasuchus figarii* (Pol et al., 2013) and *Junggarsuchus sloani* (Clark, Xu, Forster, & Eberth, 2004; Clark, Xu, Forster, & Wang, 2004). *Phyllodontosuchus lufengensis* (Harris et al., 2000), *Trialestes romeri* (Lecuona et al., 2016; Reig, 1963), *Carnufex carolinensis* (Zanno et al., 2015; Drymala & Zanno, 2016) and *Redondavenator quayensis* (Nesbitt et al., 2005) are known from incomplete or poorly preserved material and their affinities are not well understood but have been referred to the "sphenosuchians" in some studies, with the exception of *Carnufex carolinensis*. Another conflictive taxon is *Terrestrisuchus* which has been considered a junior synonym of *Saltoposuchus* (e.g., Benton & Clark, 1988), or as distinct taxa (e.g., Sereno & Wild, 1992); Allen (2003) considered *Terrestrisuchus* material to be juvenile individuals of *Saltoposuchus*, but Irmis et al. (2013) disagreed and consider them separate taxa. Nesbitt (2011) considered the specimen assigned to *Hesperosuchus* by Clark et al. (2001), CM 29894, to potentially belong to a different taxon due to its younger age within the Chinle Formation and the lack of autapomorphies shared by this specimen and the holotype of *Hesperosuchus agilis*, but Leardi et al. (2017) disputed some supposed differences between this specimen and the *H. agilis* holotype.

Many of the features shared by non-crocodyliform crocodylomorphs, like their long, gracile limbs positioned under their body, are related to an upright posture and terrestrial lifestyle, unlike living semi-aquatic crocodylians (Crush, 1984; Parrish, 1991; Sereno & Wild, 1992; Walker, 1970). However, there are few putative synapomorphies; thus, it is unclear whether or not these taxa comprise a monophyletic group. Analyses have shown the group either to be monophyletic (Clark et al., 2001; Sereno & Wild, 1992; Sues et al., 2003; Wu & Chatterjee, 1993) or paraphyletic, with some taxa being more closely related to Crocodyliformes (Benton & Clark, 1988; Clark & Sues, 2002; Clark, Xu, Forster, & Wang, 2004; Leardi et al., 2017; Nesbitt, 2011; Parrish, 1991; Pol et al., 2013; Zanno et al., 2015).

Early studies were not consistent with the use of their characters, however, and a critical review by Clark et al. (2001) revealed numerous problematic characters in earlier publications diminishing support for their results. A subsequent analysis (Clark, Xu, Forster, & Wang, 2004), including new characters and *J. sloani*, found in favor of a paraphyletic "Sphenosuchia" but with weak support. In an analysis without *Junggarsuchus*, Nesbitt (2011) also found a paraphyletic "Sphenosuchia," and more resolution among them, but with lesser taxonomic sampling. Results based on the Clark, Xu, Forster, and Wang (2004) data set, but with expanded taxon and character sampling (Leardi et al., 2017; Pol et al., 2013) have obtained similar results.

Here, the holotype specimen of *J. sloani*, IVPP 14010 (Figure 1), from the Middle-Upper Jurassic Shishugou Formation of China, is described in detail in comparison with other non-crocodyliform crocodylomorphs including detailed comparison to *D. elaphros*. The Shishugou Formation of Xinjiang (China) is a continuous series of sediments spanning the late Middle to early Late Jurassic (Clark et al., 2006; Eberth et al., 2001). The lower part of the formation has yielded a variety of turtles, brachyopoid amphibians, a mammaliaform, and theropod and sauropod dinosaurs; whereas the upper contains a more diverse fauna of dinosaurs and non-dinosaurian amniotes (Clark, Xu, Forster, & Eberth, 2004). An expedition in 2001 recovered the skull

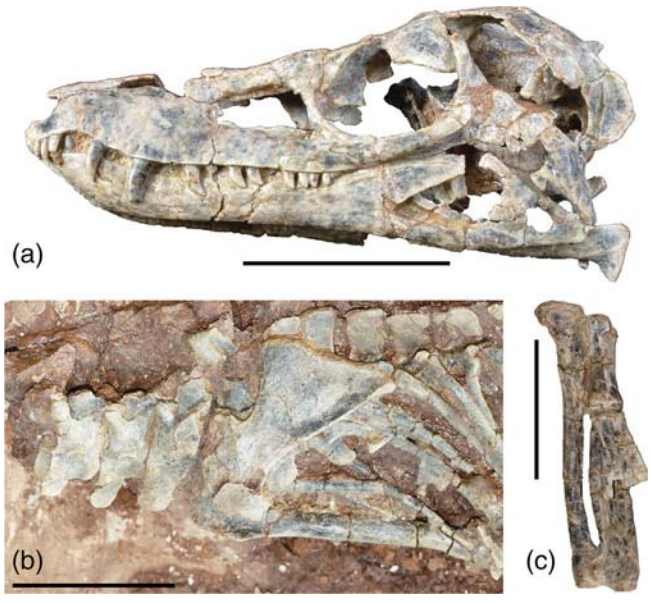

FIGURE 1 The holotype material of *Junggarsuchus sloani*: (a) the skull of *Junggarsuchus* in left lateral view; (b) the posterior cervical vertebrae and pectoral girdle of *Junggarsuchus* in left lateral view in the block; (c) the right forelimb of *Junggarsuchus* in right lateral view. Labels and details of these elements are shown in the following figures. Scale bar is equal to 5 cm.

and part of the postcranial skeleton of *J. sloani* as named by Clark, Xu, Forster, and Eberth (2004) and Clark, Xu, Forster, and Wang (2004), from the lower part of the Shishugou Formation. It was originally considered to be late Middle Jurassic (Clark, Xu, Forster, & Eberth, 2004; Clark, Xu, Forster, & Wang, 2004) based on the Gradstein et al. (2004) time scale, but later revisions (Gradstein et al., 2012) moved this boundary and indicate *Junggarsuchus* is earliest Late Jurassic (see Horizon and Locality below).

The holotype specimen consists of an exceptionally preserved skull and the anterior portion of the body, with a few disarticulated elements of the posterior portion of the skeleton that were recovered associated with the holotype (Figure 1). The holotype is the only significant specimen of *J. sloani* and was described briefly in a paper by Clark, Xu, Forster, & Wang (2004) which focused specifically on the features of the braincase and forelimbs. An initial detailed description of much of the known material of *J. sloani* was prepared by a Masters student working with Clark (Klein, 2007) but did not include CT scans. *J. sloani* has several features that reduce the morphological gap between more early diverging crocodylomorphs and crocodyliforms, including the contact of the ventral shaft of the quadrate to the otoccipital on the occipital surface of the braincase that is a key step in the beginning of the solidification of the skull (Clark, Xu, Forster, & Wang, 2004; Pol et al., 2013). We describe the external and internal anatomy of *Junggarsuchus* here using observations from CT data, including a detailed description of the palate, inner ear and braincase of *Junggarsuchus*. Previous detailed descriptions of sphenosuchian braincases have either lacked CT data and so were limited in some respects to breaks through which observations could be made (Walker, 1990; Wu & Chatterjee, 1993) or described incompletely preserved taxa (Leardi et al., 2020). *Junggarsuchus*, however, preserves nearly all aspects of the skull, and with the availability of CT data, it is one of the most completely known sphenosuchians to date.

D. elaphros is known from excellent material, including a nearly complete skull and much of the postcranial skeleton. *D. elaphros* is from the Zhangjiawa Member of the Lufeng Formation in Yunnan, China, which has been biostratigraphically dated as Early Jurassic, possibly Sinemurian (Fang et al., 2000; Luo & Wu, 1994). Several specimens are known, though the most complete is IVPP V 7907, comprising a complete skull, the anterior portion of the axial skeleton, the forelimbs and includes some elements of the hind limbs and pubis (Wu & Chatterjee, 1993). It was thoroughly described by Wu and Chatterjee (1993), but the skull has not previously been CT scanned.

Past analyses recover a similar pattern of relationships within Crocodylomorpha, in which *D. elaphros* and *J. sloani* are found to be closer to Crocodyliformes than are most other non-crocodyliform crocodylomorphs (Benton & Clark, 1988; Leardi et al., 2017; Pol et al., 2013; Wilberg, 2015), though not as close as *Macelognathus*, *Almadasuchus* and possibly *Kayentasuchus* (Wilberg, 2015). Although *Dibothrosuchus* and *Junggarsuchus* are two of the best represented members of this lineage of crocodylomorphs, there is limited comparison of these two, relatively closely related taxa, which this description improves upon.

The characters used in previous analyses are critically reviewed and reanalyzed, and the results support a paraphyletic Sphenosuchia. To better understand the evolution of important crocodylomorph characters and the relationships of *Junggarsuchus*, we have assembled the largest early diverging crocodylomorph character matrix currently in the literature, building on the most recent matrices of Leardi et al. (2017) and Wilberg (2015). Our sampling includes all currently described early diverging crocodylomorphs and 513 characters that cover important cranial and postcranial anatomy. We performed parsimony analyses with four different rooting taxa (*Gracilisuchus*, *Stagonolepis*, *Saurosuchus*, and *Postosuchus*) and weighting schemes (no implied weights, $k = 6, 12, 24$) to see how such variations might change tree topology and what this variation might tell us about how homoplastic character states affect some relationships. Taxa of particular interest to this analysis are those non-crocodyliform crocodylomorphs potentially closest to Crocodyliformes, including *Macelognathus* (Leardi et al., 2017), *Almadasuchus* (Pol et al., 2013), *Kayentasuchus* (Clark & Sues, 2002), and the marine thalattosuchians.

J. sloani, *Macelognathus vagans*, and *Almadasuchus figarii* are found to be the closest relatives of Crocodyliformes in most recent analyses, and species such as *Sphenosuchus acutus*, *D. elaphros*, *Terrestrisuchus gracilis*, and *Litargosuchus leptorhynchus* are usually found to have diverged earlier within Crocodylomorpha (Benton & Clark, 1988; Leardi et al., 2017; Pol et al., 2013; Wilberg, 2015). *Kayentasuchus walkeri*, a crocodylomorph from the Early Jurassic of Arizona (Clark & Sues, 2002), has been found in some analyses (e.g., Nesbitt, 2011) to be the sister taxon to Crocodyliformes, although *Junggarsuchus*, *Almadasuchus*, and *Macelognathus* were not included. This placement for *Kayentasuchus* as the sister taxon to Crocodyliformes was also found by later authors including Wilberg (2015), who included *Almadasuchus* and *Junggarsuchus*, and Zanno et al. (2015), who included *Junggarsuchus* though not *Almadasuchus* or *Macelognathus*. Although Wilberg's sampling included more crocodylomorph outgroup taxa, he noted that this position is not well supported, and two-character state changes would place *Junggarsuchus* and

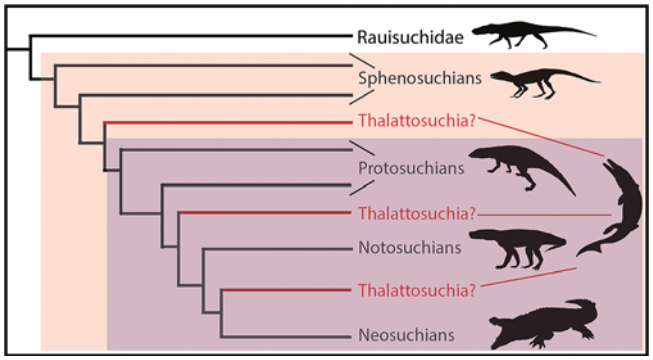

FIGURE 2 Generalized tree of crocodylomorph relationships. Thalattosuchia is placed in two positions within Crocodyliformes, and as the sister group to crocodyliforms. Sphenosuchians and protosuchians shown as paraphyletic groups. The three hypothesized placements of Thalattosuchia are in red. Crocodyliformes in purple and Crocodylomorpha in orange

Almadasuchus as sister to Crocodyliformes +- Thalattosuchia. We find *Kayentasuchus* in an earlier diverging position, a result that is consistent with the more recent results of some other researchers (Leardi et al., 2017) (see Discussion).

A further area of interest is the relationships of thalattosuchians, a group including the most highly specialized pelagic crocodylomorphs. Their relationships were considered to be obscured by homoplastic similarities with other marine crocodylomorphs (Clark, 1994; Sadleir & Makovicky, 2008), and they were placed either in their traditional position at the base of the Mesoeucrocodylia or grouped with other long-snouted taxa (Figure 2). However, Wilberg (2015) found many of the features related to a long snout to be homoplastic, and his analysis placed thalattosuchians as the sister-group of crocodyliforms, a position also discussed by Benton and Clark (1988).

2 | MATERIALS AND METHODS

The limb bones of *J. sloani* are described as if the animal was standing erect (Pol and Norell 2004). Hence, anterior = cranial and posterior = caudal. The terms "ventral" and "dorsal" are used in describing the digits but not the more proximal elements, assuming a digitigrades stance. The skull was separated from the rest of the skeleton and was transported to The George Washington University (Washington, DC, USA) for study and further prepared after the publication of Clark, Xu, Forster, and Wang (2004) and Clark, Xu, Forster, and Eberth (2004), and nearly all of the matrix was removed. Regarding the postcranial skeleton, only the left side of the skeleton has been prepared out of its plaster jacket, and the right side of the specimen has not been viewed except for the right forelimb (Figure 1a). The holotype skull was first CT scanned before extensive internal preparation on September 28, 2004 on a GE Lightspeed 16 CT scanner at Stony Brook University. The specimen was scanned at 140 kV and 160 mA with a slice spacing of 0.31 mm. Slices were reconstructed at a diameter of 96.0 mm using the GE BonePlus algorithm. The holotype skull was rescanned after nearly all of the matrix was removed in a Mi-CT 225 kV micro-computerized tomography scanner (developed by the Institute of High Energy Physics, Chinese Academy of Sciences) at the Key Laboratory of Vertebrate Evolution and Human Origins, IVPP. Slices were spaced at 0.0459 mm for a total of 3,402 slices along a 141.32-mm-long skull. We used Mimics software (Mimics Software, n.d.) (https://www.materialsise.com/en/medical/software/mimics) to segment and analyze the second CT scans of the skull. All nonphotograph illustrations of *Junggarsuchus* in this article are detailed 3D models of the masks reconstructed in Mimics and VG Studios. Additional analysis of the CT data, including the imaging of the lacrimal ducts, trigeminal nerve pathways and the generation of isosurface renders of incomplete elements was completed at Yale University, in the Bhullar Lab, using VG Studios Max Version 3.5 (VG Studio Max 3.5 (Volume Graphics), 2019).

The skull of *D. elaphros* (IVPP V7907) was CT scanned at the IVPP in Beijing using the same scanner. The rostrum and jaw were segmented in a single file, and the braincase was segmented separately, as the braincase was disarticulated from the rest of the skull. The nonphoto illustrations of the skull of *Dibothrosuchus* used in our description were all also reconstructed from Mimics and VG Studio files. Slices for the rostrum were spaced at 0.19 mm for a total of 2,881 slices along a 164-mm-long skull. Slices for the braincase were spaced at 0.19 mm for a total of 1,481 slices along a 41-mm-long skull.

Characters: The characters used in previous analyses of early diverging crocodylomorphs have been critically reviewed and reanalyzed. The final character set of 513 characters is mostly a combination of characters from Wilberg (2015, 2017), from which 290 of the characters are taken from the former and 7 from the latter, and Leardi et al. (2017), from which we included 129 characters. An additional 69 characters for crocodyliforms were taken from a data set assembled by Tennant et al. (2016), and an additional 8 and 2 characters for thalattosuchians were taken from Young and Andrade (2009) and Young et al., 2012, respectively, (Supplementary information S1 is our revised list of characters, which notes the original matrix that each character was taken from in parentheses). One modified character (Char. 395) was included

from Clark (1994). For each data set, we looked at overlap between the characters and omitted repetitive, semantically dependent characters between the data sets (Supplementary information S1 includes a list of justifications for omissions). Additionally, some characters and scorings were edited in our assembly of this new dataset and a list of these changes can be found in our supplementary material S1. In addition to the 506 characters from previous authors, we included seven new characters that detail additional morphology of the pterygoid (Char. 283), the mandibular fenestra (Char. 321), the dentary (Char. 325), the angular (Char. 348), the prearticular (Chars. 351), the articular (Char. 356), and the dentition (Char. 395). This analysis included 41 ordered (additive) characters (indicated in a nexus file and .tnt file in Supplementary information S1).

Taxa: For most taxa, we used codings taken from existing matrices, including Wilberg (2015), Leardi et al. (2017), and Young and Andrade (2009). *J. sloani* (IVPP V14010) and *D. elaphros* (IVPP V7907) were studied in person and in CT segmentation, whereas *Hesperosuchus agilis* (AMNH 6758), *Kayentasuchus walkeri* (UCMP 131830), *Hallopus victor* (YPM 1914), *Nominosuchus matutinus* (IVPP V14392), *Protosuchus haughtoni* (BP-14746, BP/1/4770), an unnamed protosuchid (UCMP 97638/125871), *Zaraasuchus shepardi* (IGM 100/1321), *Shamosuchus djadochtaensis* (IGM 100/1195), *Gavialis gangeticus*, *Crocodylus niloticus*, and *Alligator mississippiensis* were all studied in person without CT data.

Our sampling of non-crocodyliform crocodylomorphs includes 16 species. Two crocodylomorphs of uncertain relationship, *Trialestes romeri* (Lecuona et al., 2016) and *Phyllodontosuchus lufengensis* (Harris et al., 2000), were included. Our sampling of outgroup taxa outside of non-crocodyliform crocodylomorphs includes *Dyoplax arenaceus* (Maisch et al., 2013), *Erpetosuchus granti* (Olsen et al., 2000), *Gracilisuchus stipanicicorum* (Butler et al., 2014; Lecuona et al., 2017; Romer, 1972), two additional gracilisuchids (*Yonghesuchus sangbiensis* (Butler et al., 2014) and *Turfanosuchus dabensis* (Butler et al., 2014; Wu & Russell, 2001), *Postosuchus kirkpatricki* (Chatterjee, 1985; Weinbaum, 2013), *Postosuchus alisonae* (Peyer et al., 2008), *Saurosuchus galilei* (Alcober, 2000; Sill, 1974), *Stagonolepis robertsoni* (Walker, 1961) and *Effigia okeeffeae* (Nesbitt, 2007). Our ingroup sampling was more limited, with 12 species of early diverging crocodyliforms, one early diverging mesoeucrocodylian, six thalattosuchians, two notosuchians, three tethysuchians, *Calsoyasuchus valliceps* (usually placed with goniopholidids; Tykoski et al., 2002, but recently placed with *Hsisosuchus* by Wilberg et al. (2019)), one paralligatorid, and three extant crocodylians: *Alligator mississippiensis*, *Crocodylus niloticus*, and *Gavialis gangeticus*. For the complete list of taxa, see Table 1 and for their scorings see (Supplementary Data S1- on Dryad, link included in "Data Availability" statement).

Rooting: This study uses four alternative rooting schemes which vary along with the sampling of outgroup taxa (Tables 2, 3, 5), as outgroup selection has been shown to have significant effects on the ingroup topology (Wilberg, 2015). Outgroups include *Gracilisuchus*, *Stagonolepis*, *Saurosuchus* and *Postosuchus*, representatives of groups found by Nesbitt (2011) to be close to crocodylomorphs, in the order found in his analysis. When the rooting taxon was changed, taxa that have been found outside the root were excluded. The rooting schemes were varied to examine the effect of outgroup selection on ingroup topology.

Outgroup taxa were selected that had been used in analyses of early diverging crocodylomorphs in past analyses (Clark, Xu, Forster, & Wang, 2004; Leardi et al., 2017; Wilberg, 2015; Wu & Chatterjee, 1993). Rooting strategy 1 uses *Gracilisuchus stipanicicorum*, a presumed relative of early crocodylomorphs in some analyses that is often used as the rooting taxa in phylogenetic analyses of crocodylomorphs (Nesbitt, 2011; Wilberg, 2015). When rooted on *Gracilisuchus*, two other gracilisuchids, two erpetosuchids, *Stagonolepis*, *Effigia*, *Saurosuchus*, and *Postosuchus alisonae* are also included in the outgroup. The two other gracilisuchids, *Yonghesuchus sangbiensis*, and *Turfanosuchus dabenensis*, are both from the Middle Triassic of China (Wu et al., 2001; Wu & Russell, 2001). However, due to their uncertain phylogenetic position and convergence with crocodylomorphs in their small, gracile forms (Nesbitt, 2011), three other rooting schemes were implemented with gracilisuchids excluded and rooted on other taxa. Rooting strategy 2 uses *Stagonolepis robertsoni*, which is a representative of the armored, Triassic aetosaurs, a group that have been consistently found as one of the most early diverging pseudosuchians (Nesbitt, 2011). *Effigia* was included in the outgroup as a representative of Poposauroidea due to the relative completeness of the specimen and its comprehensive description (Nesbitt, 2007), although it is very specialized. The remaining outgroup taxa were maintained with the *Stagonolepis* root (Nesbitt, 2011; Wilberg, 2015). This exclusion is maintained in all subsequent analyses. Rooting strategy 3 uses the early diverging loricatan *Saurosuchus galilei*, which has consistently been found closer to crocodylomorphs than gracilisuchids, erpetosuchids, and aetosaurs (Nesbitt, 2011). Aetosaurs and poposaurs were omitted from this round of analyses over concerns that the armored herbivorous and bipedal herbivorous pseudosuchians may be too specialized as a rooting taxon and affect character polarity. *Dyoplax* and *Erpetosuchus* (erpetosuchids) were also omitted in the analyses rooted on *Saurosuchus* and *Postosuchus*. Like gracilisuchids they are of uncertain phylogenetic position and all positions are outside

TABLE 1 List of taxa used in comparison for the text and in our phylogenetic analyses

Taxon	Source
Gracilisuchus stipanicorum	Romer (1972), Butler et al. (2014), and Lecuona et al. (2017)
Turfanosuchus dabensis	Young (1973), Wu and Russell (2001) and Butler et al. (2014)
Yonghesuchus sangbiensis	Butler et al. (2014)
Erpetosuchus granti	Olsen et al. (2000) and Newton (1894)
Dyoplax arenaceus	Maisch et al. (2013)
Stagonolepis robertsoni	Walker (1961) and Gow and Kitching (1988)
Effigia okeefeae	Nesbitt (2007)
Saurosuchus galeli	Sill (1974) and Alcober (2000)
Postosuchus alisonae	Peyer et al. (2008)
Postosuchus kirkpatricki	Chatterjee (1985) and Weinbaum (2013)
Carnufex carolinesis	Zanno et al. (2015) and Dtymala and Zanno (2016)
Phyllodontosuchus lufengensis	Harris et al. (2000)
Pseudhesperosuchus jachaleri	Bonaparte (1971)
Redondavenator quayensis	Nesbitt et al. (2005)
Trialestes romeri	Lecuona et al. (2016)
Terrestrisuchus gracilis	Crush (1984) and Allen (2003)
Hesperosuchus "*agilis*" (CM 29894)	Clark and Sues (2002)
Hesperosuchus agilis (Holotype)	AMNH FR 6758
Litargosuchus leptorhynchus	BP/1/5237; Clark and Sues (2002)
Dromicosuchus grallator	Sues et al. (2003)
Kayentasuchus walker	UCMP 131830; Clark and Sues (2002)
Sphenosuchus acutus	Walker (1990)
Dibothrosuchus elaphros	IVPP V 7907; Wu and Chatterjee (1993)
Hallopus victor	YPM 1914
Junggarsuchus sloani	IVPP V 14010
Macelognathus vagans	YPM VP 001415; Leardi et al. (2017)
Almadasuchus figarii	Pol et al. (2013) and Leardi et al. (2020)
Protosuchus richardsoni	AMNH 3024; UCMP 130860; MCZ 6727 limited CT data Clark (1986)
Protosuchus haughtoni	BP/1/4770; Gow (2000)
Gomphosuchus wellsi	UCMP-97638/125871
Orthosuchus stormbergi	Nash (1975)
Hemiprotosuchus leali	Bonaparte (1969)
Gobiosuchus kielanae	Osmólska et al. (1997)
Zosuchus davidsoni	IGM 100/1305; Pol and Norell (2004a)
Zaraasuchus shepardi	IGM 100/1321; Pol and Norell (2004b)
Nominosuchus matutinus	Storrs and Efimov (2000)
Fruitachampsa callisoni	Clark (2011)
Sichuanosuchus shuhanensis	Wu et al. (1997)
Shantungosuchus hangjiensis	Wu et al. (1994)
Hsisosuchus chungkingensis	Li et al. (1994)
Steneosaurus bollensis	Herrera et al. (2018)
Metriorhynchus superciliosus	Andrews (1913)
Cricosaurus araucanensis	Herrera et al. (2018)

TABLE 1 (Continued)

Taxon	Source
Geosaurus suevicus	Young and Andrade (2009)
Dakosaurus andiniensis	Pol and Gasparini (2009)
Pelagosaurus typus	Pierce and Benton (2006)
Simosuchus clarki	Kley et al. (2010)
Baurusuchus salgadoensis	Nascimento and Zaher (2010)
Goniopholis simus	De Andrade et al. (2011)
Calsoyasuchus valliceps	Tykoski et al. (2002)
Sarcosuchus imperator	Sereno et al. (2001)
Pholidosaurus purbeckensis	Mansel-Pleydell (1888) and Andrews (1913)
Dyrosaurus phosphaticus	Jouve (2005) and Jouve et al. (2006)
Shamosaurus djadochtaensis	IGM 100/1195; Turner (2015)
Gavialis gangetics	YPM HERR 010514
Crocodylus niloticus	YPM HERR 010521
Alligator mississippiensis	YPM HERR 16540; Dufeau and Witmer (2015)

Postosuchus + Crocodylomorpha (Nesbitt, 2011), including some positions well outside the node that unites even Gracilisuchidae with other close relatives of crocodylomorphs (Nesbitt, 2011). Rooting strategy 4 uses the rauisuchid *Postosuchus kirkpatricki*, which has consistently been recovered as either the sister to crocodylomorphs or very close and is commonly included as an outgroup of crocodylomorphs (Nesbitt, 2011). This scheme has the most limited outgroup sampling.

Parsimony analysis: For this project, 16 phylogenetic trees were constructed with parsimony analysis using 513 characters applied to 57 taxa with *Gracilisuchus* as the outgroup, 54 with *Stagonolepis* as the outgroup, 50 with *Saurosuchus* as the outgroup, and 48 with *Postosuchus* as the outgroup. TNT v1.5 (Goloboff & Catalano, 2016) was used to find the most parsimonious trees and the strict consensus. Forty-one multistate characters were treated as ordered. These 41 characters were originally treated as ordered in the matrices they were sampled from. Sixteen different analyses were run with characters ordered, four for each rooting scheme. Of these four analyses, one of the tests used equal weighting, the others used implied weights of $k = 12$, as simulation studies when the true tree was known outperformed others when homoplasy was more severely downweighted (Goloboff, 1993; Goloboff et al., 2017). The second and third set of implied weight analyses was carried out at the higher and lower k value ($k = 24$ and $k = 6$) to test the data sets sensitivity to decreased and increased downweighting of homoplastic characters. While ordering of characters is justified by the similarities among the states (Lipscomb, 1992), an additional 16 analyses were carried out with no ordered characters for comparison with other analyses that did not order the characters (e.g., Wu & Chatterjee, 1993). These analyses produce divergent results in which "Sphenosuchia" is found as a monophyletic clade even in equal weight analyses when Rooting Schemes 1 or 2 are used, though results when rooted on *Saurosuchus* and *Postosuchus* are similar to those found when 41 characters are ordered. Results of these analyses are discussed and the trees are figured in the supplementary data (Figures S10–S17).

For our equal weights analyses, minimal tree lengths were first found using new technologies searches. We set the search to look for the minimum tree length five times and set the initial addition sequences at 50. This search was carried out with drift, tree fusing, and sectorial search set at the default settings. Ratchet was also included in our new technologies search for all analyses with 100 total iterations. For our implied weight analysis, tree fusing, sectorial search, drift, and ratchet were maintained, but instead of finding the minimum tree length, we looked for the stabilized consensus two times, with a factor of 75, the default. For both equal weight and implied weight analyses, to ensure that all minimum tree lengths were discovered, all analyses were subjected to traditional search with tree bisection reconnection (TBR) branch swapping. Following the use of the TBR algorithm, a strict consensus was found for the set of trees retained from the analysis. For trees with equal weights, the consistency index and retention index were calculated for each set of most parsimonious trees (Table 2).

	Gracilisuchus	*Stagonoelpis*	*Saurosuchus*	*Postosuchus*
CI	0.315	0.328	0.358	0.368
RI	0.613	0.639	0.6984	0.7
Steps	1968	1888	1731	1,686
Max	4,133	4,133	4,133	4,133
Min	620	620	620	620

TABLE 2 CI, RI, and step for equal weight analyses

Note: Taxa in column heads are for rooting scheme.
Abbreviations: CI consistency index; RI retention index.

Synapomorphies: Synapomorphies were first mapped along trees using TNT. The synapomorphies were then checked against a tree built in Mesquite (Maddison & Maddison, 2005) from our data set to visualize the evolutionary history of the character and its ambiguous and unambiguous optimizations. Synapomorphies for the groups are presented in Table 3.

Node support: Support for the nodes was found using symmetric resampling (Goloboff et al., 2003), with a .33 change probability, the default. The results for the topologies were output as both absolute frequencies and frequency differences. Frequency differences tend to give slightly lower numbers but are considered more accurate as they compare the frequency of a given group versus the frequency of the next most likely group to be found. This tests the assumed group against possible contradictory groups (Goloboff et al., 2003). This resampling was run with 100 replicates and was set to collapse any node with a support number lower than 1. Trees were searched with a new technology search, which used sectorial searches, ratchet, tree fusing, and drift and inserted an additional 10 sequences as the starting point for each analysis prior to a new technology search. The minimum length was calculated only once.

2.1 | Institutional abbreviations

AMNH: American Museum of Natural History (Fossil Reptiles), New York, USA
BP: Evolutionary Studies Institute (formerly Bernard Price Institute for Palaeontological Research), University of the Witwatersrand, Johannesburg, REPUBLIC OF SOUTH AFRICA
CM: Carnegie Museum of Natural History, Pittsburg, PA USA
CUP: Fujen Catholic University of Peking (Beijing) collection in Field Museum of Natural History, Chicago IL USA
IGM: Institute of Geology, Mongolian Academy of Sciences, MONGOLIA
IVPP: Institute of Vertebrate Paleontology and Paleoanthropology, Chinese Academy of Sciences, Beijing, China
MCZ: Museum of Comparative Zoology, Harvard, Cambridge, MA USA
UCMP: University of California Museum of Paleontology, Berkeley, CA, USA

2.2 | Abbreviations

adpq: anterior dorsal process of the quadrate
adq: suture for dorsal head of the quadrate on the prootic
ahq: articular head of the quadrate
ajp: anterior process of the jugal
anf: antorbital fenestra
angb angular
antf: antorbital fossa
antr: anterior tympanic recess
aor: anterior orbital artery
aoto: suture for otoccipital on prootic
apf?: possible additional palatine fenestra
apf: anterior prootic foramen
apl: anterior process of the palatine
apt: anterior process of the pterygoid
ar: articular
as: suture of prootic on squamosal
aoto: region of the squamosal which articulates with the paraoccipital process of the otoccipital
aso: suture of prootic with supraoccipital
at: atlas
atc: atlas centrum
atf: anterior temporal foramen
atin: atlas intercentrum
atna: atlas neural arch
atns: atlas neural spine
atoa: anterior exit of the temporo-orbital artery
atr: atlas rib
ax: axis
bc: internal space of the braincase
bib: break for internarial bar
bo: basioccipital
boc: basioccipital condyle
borss: basioccipital recess sensu stricto
bot: basioccipital tubers

TABLE 3 Unambiguous synapomorphies for groups found in each analysis where the clade is recovered.

Group	Synapomorphies
'Sphenosuchia' monophyletic: 5/16	10(0)*, 15(0), 24(0), 35(0), 80(1), 110(1)*, 139(0), 152(3)*, 212(1)*, 222(1)*, 232(0), 234(1), 256(1)*, 283(0), 346(2), 357(1), 409(1), 412(1)*, 427(1), 431(1), 436(1), 455(1), 474(1)*,
Litargosuchus + *Terrestrisuchus*: 6/16	7(2)*, 12(0)*, 13(1)*, 82(1)*, 110(1)*, 142(0)*, 165(1), 170(1), 194(0)*, 325(1), 348(1)
Redondavenator + *Kayentasuchus*: 1/16	375(0), 385(0)
Sphenosuchus + *Hesperosuchus*: 1/16	147(1), 149(1), 155(1), 345(1)
Dibothrosuchus + *Sphenosuchus*: 3/16	51(2), 142(1), 147(1), 170(1)*, 268(1), 315(1), 368(0)
(*Dibothrosuchus* + *Sphenosuchus*) + (*Hallopus* + *Solidocrania*): 3/16	13(0), 26(0), 82(0), 157(1), 173(1), 192(1), 195(1), 205(1), 276(0), 305(1), 409(2)
Sphenosuchus + (*Dibothrosuchus* + *Solidocrania*): 6/16	13(0), 82(0), 192(1), 195(1), 205(1), 409(2)
Dibothrosuchus + *Solidocrania*: 13/16	7(1)*, 13(0)*, 82(0)*, 157(1), 158(1), 173(1), 191(1), 192(2)*, 195(1)*, 202(1), 305(1), 411(1)
Dibothrosuchus autapomorphies	10(1), 17(1)*, 24(2)*, 27(1)*, 51(2)*, 116(1), 137(1)*, 158(1)*, 188(0)*, 191(1)*, 256(2)*, 338(1)*, 468(0)*, 479(0)*, 499(1), 510(0)*
Junggarsuchus autapomorphies	9(1), 61(2), 67(0), 86(1)*, 93(1)*, 97(1), 98(1), 111(1)*, 128(1), 170(0)*, 188(0)*, 206(1), 224(1), 322(1), 337(1), 338(1)*, 339(1), 433(1), 434(1), 498(1), 500(4), 501(1)
Junggarsuchus + *Phyllodontosuchus*: 5/16	97(1), 98(1), 110(1)*, 111(1)*, 325(0)
Hallopus + Solidocrania: 8/16	427(0), 429(2), 452(1), 453(1)
'Solidocrania': 11/16 paraphyletic; 5/16 in monophyletic Sphenosuchia	11(1), 86(1), 139(1)*,140(1), 174(1), 175(2), 207(2), 236(2)*, 237(1), 270(1), 285(1), 296(0), 403(1), 422(1)
Hallopodidae: 3/16	452(2), 453(1), 454(0)*
Macelognathus + Almadasuchus: 3/16	206(0), 207(3), 465(0)
Hallopodidae + Crocodyliformes: 3/16	46(1), 47(0), 142(0), 171(1), 191*(1), 210(1), 232(1), 247(1), 249(1), 267(1), 357(0), 365(1)
Macelognathus + (*Almadasuchus* + *Crocodyliformes*): 8/16	75(1)*, 142(0)*, 210(1), 232(1), 249(1), 365(1)
Almadasuchus + Crocodyliformes: 8/16	35(2), 46(1), 47(0), 48(1), 171(1), 212(0), 220(1)*, 247(1), 267(1), 357(0), 456(0)*, 460(0)*
Crocodyliformes: 16/16	1(1)*, 19(0), 20(2), 26(2)*, 38(1)*, 44(1)*, 45(1)*, 49(1), 137(1)*, 157(0), 158(1)*, 164(1), 172(2), 173(0), 179(1)*, 181(1), 190(0)*, 194(0), 196(0), 206(1), 207(4), 208(1)*, 211(1)* 222(0), 223(1)*, 225(0)*, 234(0)*, 236(2)*, 242(1), 246(1), 259(0), 262(0)*, 263(1)*, 266(1), 271(1)*, 274(2)*, 277(1)*, 280(1)*, 282(0)*, 283(1), 284(1)*, 306(1)*, 321(0)*, 327(0)*, 336(1)*, 346(0)*, 350(1)*, 353(0)*, 368(1)*, 402(1)*, 408(1)*, 409(3), 416(1)*, 429(1)*, 432(0)*, 449(1)*, 450(1)*, 452(1)*, 453(0), 454(1)*, 455(0), 478(1)*, 491(1)*
Thalattosuchia + Crocodyliformes: 7/16	1(1)*, 2(1), 7(1), 13(0)*, 28(1)*, 30(1)*, 38(1), 44(1)*, 49(1), 58(2)*, 83(1)*, 116(1)*, 117(0)*, 124(1), 137(1)*, 147(1)*, 161(0)*, 172(2), 192(2), 195(1), 196(0), 210(1)*, 216(1), 225(0), 236(2)*, 237(1), 247(1), 259(0)*, 267(1), 271(1), 282(1), 284(1), 298(0)*, 299(1), 306(2), 361(1), 365(1)*, 408(2), 422(1), 446(1), 449(1), 450(1), 478(1), 491(1),
Hsisosuchus + Crocodyliformes: 7/16	1(1)*, 11(1)*, 15(0), 19(0), 45(1)*, 46(1), 47(0), 48(1), 86(1)*, 111(0)*, 171(1), 174(1), 175(2), 179(1), 181(1), 182(1)*, 191(1), 202(1), 207(4), 220(1), 223(1), 224(0)*, 246(1), 304(1)*, 352(1)*, 403(1), 411(0), 475(0), 479(0), 486(1)*, 490(1),
Protosuchia paraphyletic: 3/16	36(0), 50(0), 228(1), 348(1), 375(0), 385(0), 454(1)

(Continues)

TABLE 3 (Continued)

Group	Synapomorphies
Protosuchidae: 16/16	27(0)*, 36(0)*, 45(1), 67(3)*, 83(1)*, 85(0)*, 14,871)*, 174(0)*, 175(0)*, 182(0)*, 201(1)*, 209(1)*, 251(1), 274(3)*, 295(1)*, 350(0)*, 375(0)*, 385(0)*, 448(0)*, 466(0)*, 474(1)*, 508(1)*
Protosuchia monophyly: 13/16	3(0), 26(1), 67(2), 137(1), 206(1), 211(1), 262(0), 321(0), 353(0), 454(1), 486(1)
Mesoeucrocodylia (Protosuchians + Hsisosuchus): 3/16	11(2)*, 28(1), 86(0)*, 143(1)*, 170(0)*, 182(1)*, 214(1), 217(0)*, 274(2), 282(1), 305(0)*, 306(2)*, 325(2)*, 350(1)*, 416(0)*, 451(1)*, 452(0)*
Thalattosuchia: 16/16	10(1), 15(1)*, 19(1), 20(0)*, 21(1)*, 45(0)*, 46(0), 47(1), 48(0), 52(1), 66(1), 100(1), 134(1)*, 155(1)*, 158(2)*, 160(0)*, 164(1), 166(1)*, 168(0)*, 171(1)*, 174(0)*, 179(0)*, 180(0)*, 181(0)*, 184(1)*, 199(1), 207(1)*, 208(0)*, 209(0)*, 214(0)*, 220(0*), 235(0)*, 246(2)*, 248(2)*, 254(0)*, 255(0)*, 257(2)*, 258(2)*, 263(0)*, 275(1)*, 290(1)*, 304(0)*, 309(1), 327(1)*, 342(1)*, 344(1)*, 346(1)*, 348(0)*, 382(0)*, 382(0)*, 392(1)*, 402(0)*, 405(0)*, 407(1)*, 416(1)*, 424(0)*, 441(1)*, 444(0)*, 459(0)*, 465(1)*, 497(1)*, 513(1)*

Note: Number in parentheses is the character state. Ambiguous synapomorphies indicated by *.

bpt: basipterygoid process
bt: biceps tubercle
cc: crista cranii
ch: choana
ci: crista interfenestralis
cor: coronoid
corc: coracoid
cppro: crista prootica
cpt: capitate process
crn cranioquadrate canal
crt: opening for internal carotid artery
ct: centrum
ctn: chorda tympani nerve
d: dentary
dc: distal carpals
dect: dorsal process of ectopterygoid
dg: digit
dh: distal end of humerus
dia: diapophyses
dmq: dorsomedial process of quadrate on prootic
dmrap: dorsomedial process of retroarticular process
dpc: deltopectoral crest
dpf: descending process of the prefrontal
dq: dorsal head of the quadrate
dqf: dorsal quadratojugal
dr: distal end of radius
du: distal end of ulna
dvt: dorsal vestibule
ect: ectopterygoid
em: edentulous portion of the maxilla
excap: extracapsular buttress
f: frontal
fleu: foramen for the lateral eustachian tube
fmeu: median pharyngeal foramen
fpf: foramen in the prootic facial recess
fl: flocculus
fm: foramen magnum
fo: fenestra ovalis
fort: fenestra pseudorotundum
fr: frontal ridges
fro: fenestra rotunda
ftoa: fenestra for temporal orbital artery
gf glenoid fossa
h: humerus
hh: hooked head of humerus
ho: humerus oval depression on head
hri: heads of rib
hya: hyapophyses
hypf: hypophyseal fossa
ic: inner carotid
imkf: intrameckelian foramen
ir: intertympanic recess
itf: infratemporal fenestra
IV: cranial nerve 4
IX-XI: cranial nerves 9–11
j: jugal
jg: jugal ventral groove
l: lacrimal
lf: lacrimal fenestra
lg: lagena
llp: lateral lamina of the prootic
llpf: lateral lamina of the prootic foramen
lmd: lacrimal medial depression
lp: ligament pits
ls: laterosphenoid
m: maxilla

mbcf: medial braincase foramen
mc: metacarpals
mnf: mandibular fenestra
mpo: medial process of the postorbital
mpq: medial process of the quadrate
mft: metotic foramen
mnd a/v: mandibular artery or vein
mr: medial ridge of the humerus
n: nasal
na: neural arch
nf: nutrient foramina
nld: nasolacrimal duct
ns: neural spine
od: odontoid process
ol: olecranon process
op: opisthotic
or: orbit
oscc3: opening for the third semicircular canal
ost: osteoderms
oto: otoccipital
otor: otoccipital recess
otspc: otosphenoidal crest
p: parietal
pb: palpebral
pdq: posterodorsal process of the quadrate
pdt: pit for dentary tooth
pf: prefrontal
pfo: prefrontal overhang
pfap: prefrontal anterior process
pfpa: prefrontal palatine contact
pfr: prootic facial recess
pfrf: prootica facial recess foramen
ph: phalange
pi: pisiform
pl: palatine
plr: palatine rod
pm: premaxilla
po: postorbital
po2: postorbital alternate interpretation
poc: postorbital concavity
pocr: postcartoid recess
prcr: precarotid recess
pop: paroccipital process
poz: postzygapophysis
pp: postglenoid process of the coracoid
ppl: posterior process of the palatine
pqf: postquadrate foramen
prb: parabasisphenoid
prb/ls: parabasisphenoid-laterosphenoid suture
prl: proximal end of radiale
pro: prootic
prz: prezygapophysis
pt: pterygoid
ptf: posttemporal fenestra
ptp: pterygoid process
ptr: posterior tympanic recess
pul: proximal end of ulnare
q: quadrate
qf: quadrate fenestra
qj: quadratojugal
qp: pneumatic expanded region of the quadrate
qp1: dorsal pneumatic space of the quadrate
qp2: pneumatic space of the quadrate continuous with the quadrate foramen
qp3: ventromedially expanded pneumatic space of the quadrate
qrp: quadrate ramus of the pterygoid
r: radius.
rap: retroarticular process
rhomb: rhomboidal recess
ri: rib
rl: radiale
rmp: ridge for *M. pterygoideus ventralis*
r-q: right displaced quadrate
s: squamosal
s2: squamosal alternate interpretation
sa: surangular
sbng: subnarial gap
sbr: sub-basisphenoidal recess
sc scapula
scb: scapular blade
scca: anterior semicircular canal
sccp: posterior semicircular canal
sccl: lateral semicircular canal
scp: sagittal crest of the parietal
so: supraoccipital
sof: suborbital fenestra
sp: splenial
spo: supraorbital vein or artery
sqg: squamosal ventral groove
sqlc: squamosal lateral concavity
srf: surangular fenestra
stf: supratemporal fenestra
stfo: supratemporal fossa
sur/q: surangular/ quadrate
toa: temporo-orbital artery
toag: temporo-orbital artery groove
trh: tooth root hole
tri: trigeminal nerve exit
trir: trigeminal recess—this was the ventral fossa of the laterosphenoid?
trnf: elongate nutrient foramina for the mandibular branch of the trigeminal nerve
tpt: transverse process of the pterygoid
u: ulna
ul: ulnare

upr: unpreserved possible region of median pharyngeal foramen in *Junggarsuchus sloani*
v: vomer
v_2: maxillary path of the trigeminal nerve
v_3: mandibular path of the trigeminal nerve
vd displaced vomer
vg + cn: exit for cranial nerves and vagus nerve?
VII: exit for cranial nerve 7
vl: ventral process of lacrimal
vps: ventral process of the squamosal
XII: exit for cranial nerve 12

3 | SYSTEMATIC PALEONTOLOGY

Archosauria, Cope 1896
Pseudosuchia, Zittel 1887
Crocodylomorpha Hay, 1930 (*emend* Walker, 1970)

3.1 | *Dibothrosuchus* Simmons, 1965

Type species: *Dibothrosuchus elaphros* (Simmons, 1965), by original designation.

Comments: IVPP V7907 was originally described as a second species of *Dibothrosuchus*, *D. xingsuensis* (Wu, 1986), but it was synonymized with *D. elaphros* by Wu and Chatterjee (1993) and currently only the type species is recognized as valid in this genus.

3.2 | *Dibothrosuchus elaphros* Simmons, 1965

Holotype: CUP 2081, a partial skull and skeleton.
Referred specimens: IVPP V7907, a nearly complete skull and mandible and partial postcranial skeleton; Wu and Chatterjee (1993) referred three other, incomplete specimens (CUP 2106, 2084, and 2489) to this species.
Horizon and localities: The holotype and referred specimens were collected near Dawa village, about 10 km northeast of Lufeng, Yunnan (Wu & Chatterjee, 1993). They are from the Zhangjiawa Member of the Lufeng Formation (the Dark Red Beds of the Lower Lufeng Formation of Luo & Wu, 1994) following the terminology of Fang et al. (2000).
Revised diagnosis: Of the original character states in the diagnosis by Wu and Chatterjee (1993), the following remain valid: frontals with three parasagittal ridges converging at both ends; frontal–postorbital contact forming a crescentic ridge in dorsal view; and a transversely broad supratemporal fenestra, nearly 30% of the width of the skull table; pronounced oval depression on anterior surface of the humerus (may be present in *Junggarsuchus* but smaller). Wu and Chatterjee (1993) identified potential autapomorphies as uncertain due to the unknown conditions in other non-crocodyliform crocodylomorphs at the time and we find support for the following: the squamosal curves sharply medially anterior to the supratemporal fenestra; squamosal separated from quadratojugal by quadrate; elongate antorbital fenestra, over half the length of the obit, surrounded by a triangular antorbital fossa; ventral process of the postorbital covers the posteromedial surface of the jugal; a small mandibular fenestra, triangular in lateral view. The full sheathing of the basioccipital condyle by the otoccipital is not supported as an autapomorphy due to our uncertain reconstruction of that region in *Dibothrosuchus* and *Junggarsuchus*. The condition of the anterior temporal foramen is seen in *Junggarsuchus* and so rejected as an autapomorphy. The autapomorphies of the coracoid are also reported in other non-crocodyliform crocodylomorphs (Clark, Xu, Forster, & Wang, 2004). The trigeminal recess is also not supported as an autapomorphy and may be widely present in non-crocodyliform crocodylomorphs (Leardi et al., 2020). We also identified several other potential autapomorphies in *Dibothrosuchus* from our own analysis, including the lateral border of the orbit is medial to the lateral border of the supratemporal fenestra (Char. 10-1); the supratemporal fossae is sub-circular in dorsal view (Char. 17-1); the lateral temporal fenestra is over 50% the size of the orbit (Char. 24-2); the suborbital fenestra is over 50% the diameter of the orbit (Char. 27-1); the descending process of the prefrontal contacts the palatine, unlike other non-crocodyliform crocodylomorphs (Char. 116-1); the total anteroposterior length of lacrimal is equal or shorter than the anteroposterior length of the prefrontal (Char. 137-1); the postorbital bar of the postorbital is medial or posterior to jugal (Char. 158-1); a tapered and pointed distal end of the posterodorsal process of the squamosal (Char. 188-0); an anteriorly well-developed posterior shelf of the supratemporal fossa (Char. 191-1); a lack of a depression for the posterior tympanic recess (Char. 256-2); the basipterygoids are massively expanded ventrally and mediolaterally and are pneumatic (Char. 268-1); the posterior extension of the surangular pinched off anterior to the articular (Char. 338-1); a massively enlarged and pneumatic prootic and potentially ventrally closed prootic facial recess (facial antrum); the medial region of distal articular surface of the tibia extends further distally than the lateral region, forming a strongly oblique distal margin of the tibia (Char. 468-0); the anterolateral process of dorsal osteoderms is absent (Char. 479-0); all cervical neural spines are rod-like (Char. 499-1); a holocephalus rib head on the axis rib (Char. 510-0).

3.3 | Solidocrania, new taxon

Definition: The least inclusive clade including *Junggarsuchus sloani* Clark, Xu, Forster, & Wang, 2004), *Almadasuchus figarii* (Pol et al., 2013) and *Macelognathus vagans* (Marsh, 1884).

Etymology: Solidocrania is a combination of *solidum* (L., solid) and *kranion* (Gr., skull), in reference to the rigid skull of these taxa.

Diagnosis: Unambiguous synapomorphies supporting Solidocrania include: two large palpebrals (Char. 140-1); the squamosal contacts the posterodorsal surface of the quadrate enclosing the otic recess posteriorly (Char. 174-1); the quadrate, squamosal, and otoccipital enclose the cranioquadrate canal laterally (Char. 175-2); the primary head of the quadrate approaches the laterosphenoid (Char. 207-2); the otoccipital contacts the quadrate ventrolaterally (Char. 237-1); the parabasisphenoid is greatly expanded with pneumatic cavities (Char. 270-1); a developed anterior process of the ectopterygoid projecting along the medial surface of the jugal (Char. 296-0); the anterior edge of the scapular blade is larger than the posterior edge (Char. 403-1); the olecranon process of the ulna is very low (Char. 422-1). Ambiguous character states that may support group (found in Mesquite using parsimony): reduction in the size of the antorbital fenestra (Char. 11-1); the lacrimo–nasal contact is excluded by an anterior projection of the prefrontal meeting posterior projection of the maxilla (Char. 86-1); the presence of palpebral elements (Char. 139-1); the presence of an additional quadrate fenestra has been inferred as a synapomorphy of this group, and the loss of the additional fenestra in *Almadasuchus* and *Macelognathus* may be secondary losses (Char. 206-1); the otoccipitals contact ventral to the supraoccipital, which is reversed in *Almadasuchus* (Char. 236-2); and a pneumatized pterygoid (Char. 285-1).

Comments: The phylogeny of early diverging crocodylomorphs remains tentative, but the group including crocodyliforms and the taxa with a similarly reinforced skull is one that will likely be referenced repeatedly in the future. However, given the late appearance of the genera closest to Crocodyliformes, it is possible that they represent a group independent of crocodyliforms and the braincase characters are homoplastic, and the definition is phrased such that they would form a discrete group excluding crocodyliforms if that is the case.

3.4 | *Junggarsuchus* Clark, Xu, Forster, and Wang, 2004

Type Species: *Junggarsuchus sloani* (Clark, Xu, Forster, & Wang, 2004), by original designation.

3.5 | *Junggarsuchus sloani* Clark, Xu, Forster, and Wang, 2004

Holotype: IVPP14010, a nearly complete skull and mandible and the anterior part of the postcranial skeleton.

Horizon and locality: Upper part of lower Shishugou Formation, Wucaiwan, Altay Prefecture, Xinjiang, China. A tuff approximately 30 m stratigraphically above this specimen has been dated at 162.2 ± 0.2 million years (Choiniere et al., 2014), which places it younger than the 163.5 ± 4 mya estimated age of the Middle-Late Jurassic boundary (albeit with a large error; Gradstein et al., 2012). With an estimated sedimentation rate of ~4.6 cm/ka (Eberth et al., 2001), the fossil is estimated to be about 652,000 years older than the dated tuff, placing it at approximately 162.85 mya, still slightly younger than the boundary estimate.

Revised diagnosis: Autapomorphies of *J. sloani* found in all of our analyses include: Premaxilla, ventral edge is dorsal to the ventral edge of the maxilla (Char. 61-2); presence of prefrontal overhang (Char. 128-1); two quadrate fenestrae (Char. 206-1); the quadratojugal extends anteriorly forming part of the ventral edge of the infratemporal bar (Char. 224-1); the mandibular fenestra inclined anterodorsally (Char. 322-1); presence of a surangular foramen (Char. 337-1); dorsal edge of the surangular anterior to the glenoid fossa is arched dorsally (Char. 339-1); the first manus digit faces laterally (Char. 433-1); the first metacarpal is slender (Char. 434-1); well-developed hypapophyses present on cervical and anterior dorsal vertebrae (Char. 500-4); procoelous vertebral centra in the cervical vertebra (Char. 498-2) and dorsal vertebra (Char. 501-2). Depending on the relationships of *Junggarsuchus* relative to *Phyllodontosuchus*, the following may also be autapomorphies: a pit between premaxilla and maxilla for lower caniniforms not exposed laterally (Char. 67-0); the lateral edges of the nasals are oblique to one another (Char. 93-1); the jugal is arched dorsally (Char. 97-1); the ventral edge of jugal has a longitudinal concavity (Char. 98-1); the posterior process of the jugal is shorter than 50% of the anterior process (Char. 110-1); the jugal terminates just anterior to the posterior border of the infratemporal fenestra (Char. 111-1); the squamosal lacks a dorsal ridge along edge of the supratemporal fossa (Char. 170-0); the squamosal posterolateral process distal end is tapered and pointed (Char. 188-0); *M. pterygoideus ventralis* insertion extends well onto the angular (Char. 349-2). It is possible that additional fenestrations in the palate are present and the squamosal may make up the entire lateral border of the supratemporal fenestra (Char. 180-1). The presence of scleral ossicles is found as an autapomorphy (Char. 9-1), but the rarity of these structures could be due to a taphonomic bias against their preservation.

4 | DESCRIPTION OF *JUNGGARSUCHUS* AND COMPARISON WITH *DIBOTHROSUCHUS*

Nearly all of the matrix has been removed from the skull of *J. sloani* and the bone has been glued where it had separated along several large cracks. The largest of these is between the braincase and the rest of the skull, where the dorsal part of the braincase is now rotated 5 mm to the left and the ventral part was rotated anteriorly. The right posterolateral part of the skull and mandible were eroded before discovery. The quadratojugal, squamosal, postorbital, all but the anterior tip of the jugal, the paroccipital process lateral to the quadrate, much of the angular, most of the surangular except its most anterior end, and the posterior end of the splenial are missing or too fragmentary to identify. The right articular and a fragment of the angular and posterior dentary are preserved separately. The ventral portion of the right quadrate has been broken and separated from the rest of the bone and was preserved in the right orbit. The left ventrolateral part of the parabasisphenoid is missing, and both pterygoids are fragmentary. A large piece is missing from the dorsal part of the rostrum just anterior to the antorbital fenestra and another from the right laterosphenoid. The sclerotic ossicles were preserved in the right orbit and were removed in articulation, a portion of the hyoid skeleton and a portion of the right postorbital and palpebral were also removed along with numerous fragments. A fragment of a large tooth was collected on the surface. During preparation, part of the right palatine was broken off and mistakenly glued to the anterior palatal process of the pterygoid.

The postcranial skeleton was preserved largely in articulation and was prepared lying on its right side. The right side of the vertebrae and ribs and most of the right shoulder girdle are not exposed, but the incomplete right forelimb and the left, dorsal, and ventral surfaces of most vertebrae are visible. Nearly all of the elements of the left forelimb were preserved in articulation, and these were removed from the skeleton. Only three complete and four partial phalanges are preserved on the left side. The right ulna and radius are preserved with their proximal ends articulated with the humerus on the main block and the remainder in pieces separately. The disarticulated elements of the atlas were preserved with the skull, the axis and following two cervicals were removed from the block when the skull was separated, and a cervical and three posterior dorsal vertebrae were collected separately in the field. Fifteen cervical and dorsal vertebrae and nearly the entire rib cage is preserved in articulation. Osteoderms and gastralia are not preserved; an interclavicle, clavicles, and sternum are not evident, but the ventral midline of the skeleton has not been completely prepared. A distal caudal vertebra and a putative sacral rib were collected from the surface.

4.1 | Cranium

4.1.1 | Skull openings

The **antorbital fenestra** of *Junggarsuchus* (Figures 3a,b and 4a,b) is 26.9 mm long (Table 4), over a third of the length of the maxilla in lateral view, and triangular in shape, with corners anteriorly, posterodorsally, and posteroventrally. The maxilla borders the anterior, anterodorsal, and ventral sides of the fenestra. The ventral edge of the fenestra slopes posteroventrally relative to the ventral edge of the maxilla. The lacrimal borders the antorbital fenestra posteriorly and posterodorsally and as a consequence, the jugal is fully excluded from the border of the fenestra. The antorbital fenestra is smaller than the orbit in *Junggarsuchus*, which contrasts with the condition in *Dibothrosuchus* and *Sphenosuchus*, which have fenestrae nearly as large as their orbits. The fenestra is also taller and less elongate than in non-crocodyliform crocodylomorphs like *Terrestrisuchus*. The antorbital fossa is present as a dorsoventrally short lamina on the anterior, anterodorsal and anteroventral edges of the antorbital fenestra (Figure 3). The antorbital fenestra of *Junggarsuchus* is large (more than half the size of the large orbit), but not as large relative to the orbit as in other non-crocodyliform crocodylomorphs like *Dibothrosuchus* and *Sphenosuchus*. It is still large relative to the fenestra in *Protosuchus haughtoni* (BP/1/4770) and *Orthosuchus*, which have fenestrae less than 50% the length of their orbit (Brown, 1933; Nash, 1975).

The **orbit** of *Junggarsuchus* is circular and large (Figures 3a,b and 4a,b), at 37 mm long, it is over 130% the length of the 26-cm-long antorbital fenestra, and over one-fifth the length of the 14.3 cm skull. The orbit faces laterally and it is not exposed on the dorsal aspect of the skull, like *Dibothrosuchus* and other non-crocodyliform crocodylomorphs, but unlike living crocodylians, which have dorsally facing orbits (Jouve, 2009). Anteriorly, the orbit is bordered by the lacrimal, in which the posterior process contributes slightly to the medial wall of the orbit. The anterodorsal border of the orbit is formed by the prefrontal and the posterodorsal border is formed by the frontal and overlain by the palpebral. The posterior border of the orbit consists nearly entirely of postorbital. The jugal forms nearly all the ventral border of orbit, except the anterior most part. The posteroventral process of the lacrimal makes up this anteroventral border of the orbit.

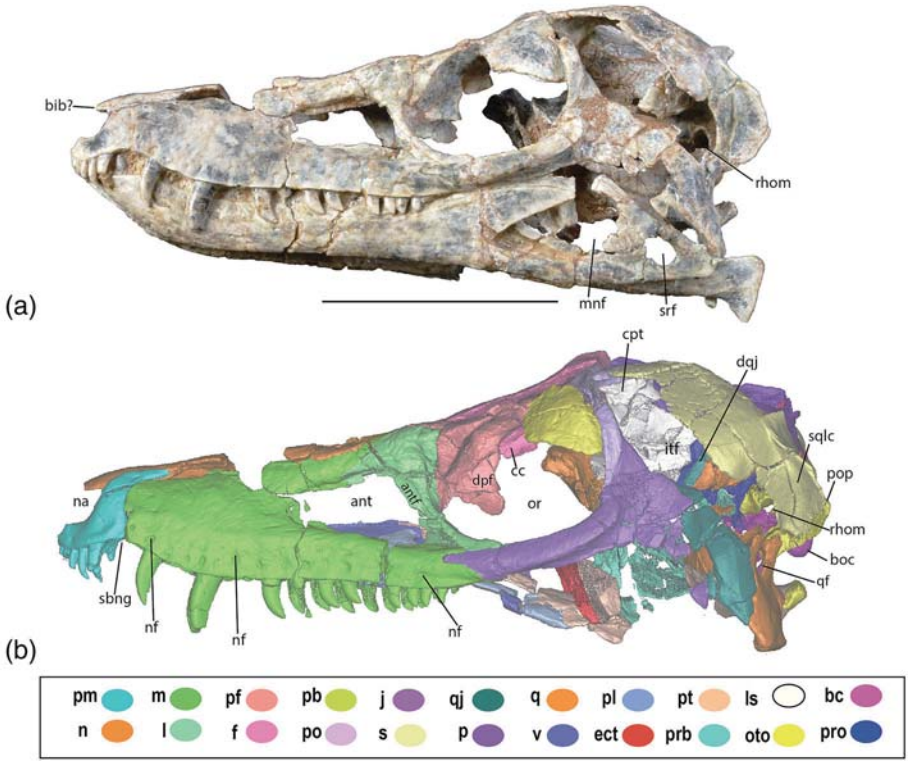

FIGURE 3 (a) Photograph and (b) CT reconstruction of the skull of *Junggarsuchus sloani* in left lateral view; scale bar is 5 cm (see list of anatomical abbreviations).

The orbit of *Dibothrosuchus* (Figures 5 and 10a) is smaller relative to the size of the skull than in *Junggarsuchus*, only roughly one-sixth the length of the skull, and smaller relative to other non-crocodyliform crocodylomorphs like *Sphenosuchus* (Walker, 1990), *Hesperosuchus agilis* (CM 29894) (Clark et al., 2001), *Terrestrisuchus* (Crush, 1984) and *Pseudhesperosuchus* (Bonaparte, 1969). In *Dibothrosuchus* and *Junggarsuchus*, the prefrontal contributes to the dorsal half of the anterior portion. In *Dibothrosuchus*, the prefrontal contributes more to the medial wall of the orbit and the jugal forms the posterior border of the orbit (Wu & Chatterjee, 1993) as opposed to the postorbital as in *Junggarsuchus*. The orbit of *Dibothrosuchus* lacks the prefrontal overhang seen in *Junggarsuchus*.

The **supratemporal fenestra** of *Junggarsuchus* is nearly one-fourth the length of the skull and is triangular (Figure 9a,b). The fenestra narrows anteriorly along with the skull table, like in *Almadasuchus*. In *Junggarsuchus*, the lateral and posterior borders of the supratemporal fenestra are formed by the parietal, whereas the squamosal contributes to the posterolateral corner and most of the lateral border. The frontal contributes slightly to the fossa but does not contribute to the fenestra. The anterior border of the supratemporal fenestra is comprised nearly entirely of the postorbital, if our primary interpretation of the postorbital is accurate (see below). Otherwise, this would imply that the squamosal borders the anterior and lateral edges and the postorbital is not involved at all, which is a condition unseen in other non-crocodyliform crocodylomorphs. The supratemporal fenestra narrows anteriorly similar to the condition observed in *Protosuchus haughtoni* (BP/1/4770) and *Protosuchus richardsoni* (Clark, 1986) and unlike the circular supratemporal fenestra in *Dibothrosuchus*.

In *Dibothrosuchus*, the supratemporal fenestra is smaller relative to the skull roof and oval with a similar axis (Figure 25d). Overall, the borders of the fenestra are largely similar, though the parietal contributes more to the posteromedial edge of the fenestra, the postorbital comprises the anterior border and the frontals contribute to the border anteriorly. In addition, *Dibothrosuchus*, unlike *Junggarsuchus*, has an anteroposteriorly elongate shelf-like supratemporal fossa that floors the posterior half of the fenestra. The prootic floors the posterior half of the fossa.

The **infratemporal fenestra** of *Junggarsuchus*, though incomplete, appears similar in shape to that of *Sphenosuchus* (Walker, 1990), as it is anteroposterior narrow and dorsoventrally tall (Figures 3a,b and 4a,b). The borders of the infratemporal fenestra in *Junggarsuchus* are not all clearly defined due to unclear sutures and incomplete jugal, quadratojugal, and postorbital. The postorbital appears to form the anterodorsal border of the fenestra. The posterodorsal border of the fenestra appears to be comprised of the squamosals. The quadratojugal forms the posterior border and some of the posterior ventral border of the fenestra. The ventral border and

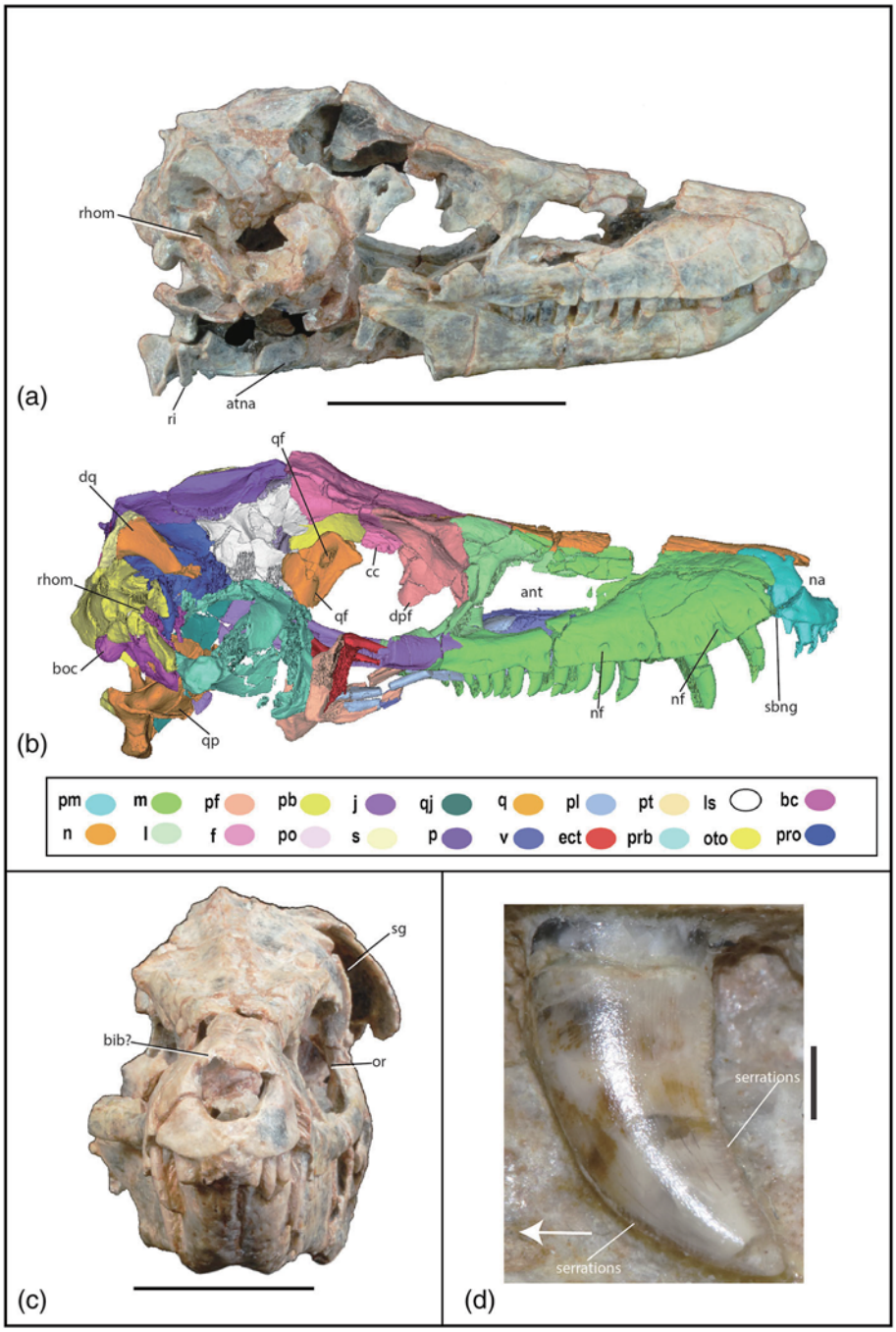

FIGURE 4 (a) Photograph of skull of *Junggarsuchus sloani* in right lateral view, and (b) CT reconstruction of skull in right lateral view; (c) skull in anterior view; (d) lateral view of fifth maxillary tooth. Scale bar is equal to 5 cm in (a), 1 cm in (c), and 2 mm in (d). Labels for maxilla neurovascular foramen indicate anterior and posterior extent of the foramina. Arrow indicates anterior direction.

anteroventral edge of the fenestra are formed by the jugal. Unlike in *Sphenosuchus*, *Protosuchus richardsoni* (AMNH 3024) and *Protosuchus haughtoni* (BP/1/4770), the jugal does extend posterior of the infratemporal fenestra.

The borders of the infratemporal fenestra of *Dibothrosuchus* are not well preserved, but the reconstruction by Wu and Chatterjee (1993) based on available material reconstructs the fenestra as longer that the orbit, unlike *Junggarsuchus*. The postorbital contributes to the entire anterior border of the fenestra and the anterior half of the dorsal border, unlike the condition in *Junggarsuchus*. Other differences include that the ventral border is comprised only of the jugal, whereas the quadratojugal only contributes to the posterior border. The ventral border of the infratemporal fenestra is flat, unlike the narrow, rounded ventral border seen in *Junggarsuchus* and *Protosuchus haughtoni* (BP/1/4770). Like *Junggarsuchus*, the posterior half of the dorsal border is comprised of the squamosal. We cannot comment further on the shape and size of this fenestra in *Dibothrosuchus* as we did not observe the holotype specimen (CUP 2081), which preserves more of this region than IVPP V7907 (Simmons, 1965).

TABLE 4 Table of measurements of the cranium and postcranium of *Junggarsuchus sloani* (IVPP 14010) in millimeter

Skull midline length	141.2
Orbit height/length	32.9/37.6
Antorbital fenestra height/length	13.9/26.9
Rostrum height at L lacrimal	31.5
Length supratemporal fenestra maximum length	32.3
Foramen magnum height/width	11.6/12
Palpebral length	15.4
Rostrum width/height at largest max tooth	24.5/26.5
Max depth of basisphenoid recess below braincase	24
Length mandibular fenestra height/length	13.9/25.9
Mandibular synthesis length	27.1
Length mandible total length	144.3
Length/height left retroarticular process	9.3/13.3
Max height of posterior mandible	23
Minimum height mandible just posterior to symphysis	11.9
Left scapula length along posterior edge (glenoid-dorsal rim)	51.8
Left scapula length along anterior edge (glenoid-anterior edge dorsal rim)	51.4
Left coracoid length (anteroproximal-posterior)	55.9
Left humerus length	105.9
Left humerus minimum shaft diameter	7.3
Left humeral deltopectoral crest length	22.9 (proximal end grades into articulation surface)
Left humerus width across distal condyles	17.8
Left radius length	94.9
Left radius minimum shaft diameter	4.9
Left ulna length	104.2
Left ulna minimum shaft diameter	4.9 (narrow region is crushed)
Left radiale length	36.2
Left ulnare length	26.7
Left metacarpal I length	20
Left metacarpal II length	24.4
Left metacarpal III length	28.3
Left metacarpal IV length	25.5
Left prox phalange length	10.9
Axis centrum length(w/o odontoid)	25
Odontoid process length	9.5
Odontoid process width	5
First articulated cervical: length centrum	18.5 (condyle length estimated)
Length/depth hypapophysis	7.2/4.1
Last articulated dorsal: centrum length	17.9
Length/height of neural spine	14.8/9.4

The **choanae** of *Junggarsuchus* are slit-like, six times as long as they are wide at the center and they narrow anteriorly and posteriorly. The maxilla borders the choanae anteriorly and anterolaterally; the vomer forms the entire medial border, and the palatines comprise the lateral and posterior edges of the choana (Figure 11c).

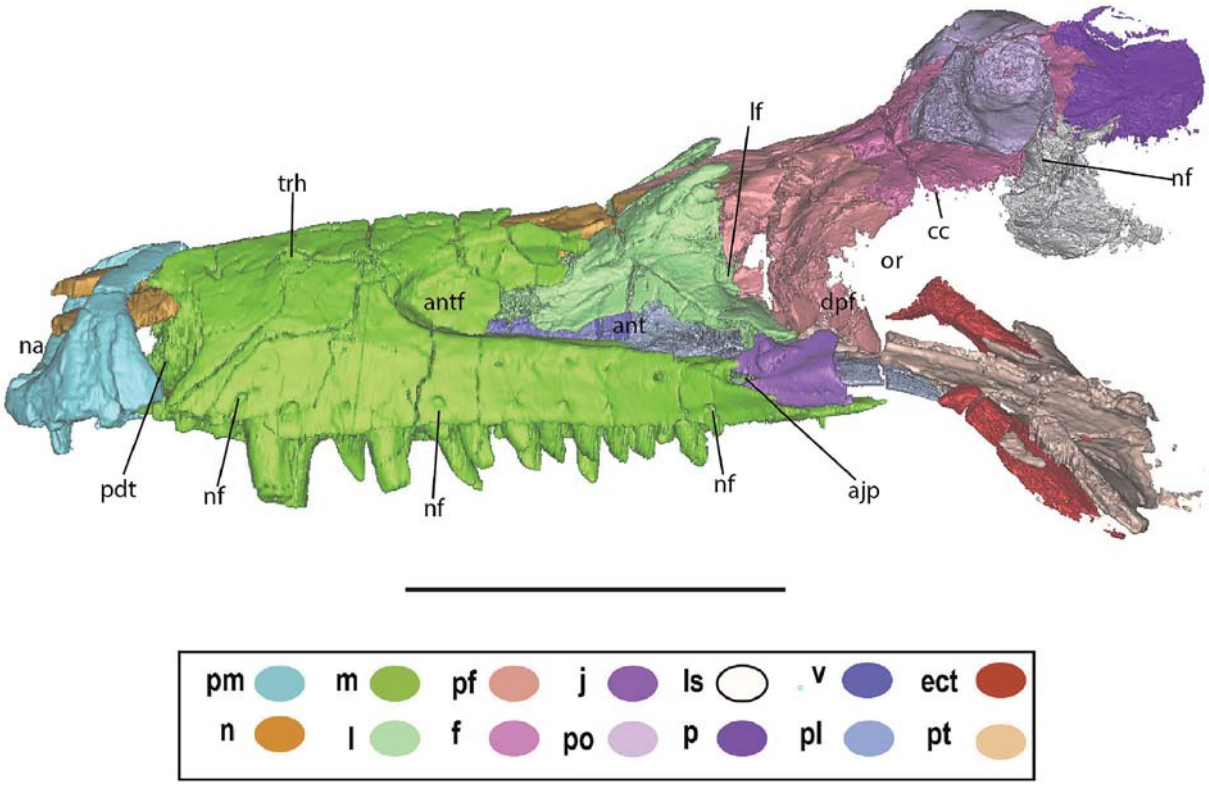

FIGURE 5 CT reconstruction of the rostrum of *Dibothrosuchus elaphros* in left lateral view; scale bar is 5 cm.

The borders of the choanae of *Dibothrosuchus* are formed by the same elements as seen in *Junggarsuchus*. The choanae themselves are slightly shorter and wider than in *Junggarsuchus*. The pterygoids are not involved with the choanae in *Junggarsuchus* unlike in crocodyliforms (Figure 11c).

The **suborbital fenestra** of *Junggarsuchus* is not clearly preserved as the incomplete palatine makes it difficult to determine the exact size of the fenestra. The anterior border of the fenestra is formed by the palatine exclusively (Figure 11a,c). A thin extension of the palatine encloses the anterior half of the lateral border of the fenestra. The anteromedial border is also comprised of the palatine. It is not clear how the pterygoid bordered the medial and posterior border of the suborbital fenestra. The posterolateral edge and part of the posterior edge are enclosed by the ectopterygoid. The fenestra appears to narrow posteriorly.

Dibothrosuchus has a large suborbital fenestra relative to the orbit, which is more oval than in other non-crocodyliform crocodylomorphs. The oval suborbital fenestrae are anteroposteriorly longer than they are mediolaterally wide, but the broken palatines do not allow us to give an exact comparison between the long and wide axes of the fenestra (Figure 11e). The borders of the fenestra are similar to those in *Junggarsuchus*. The pterygoid contributes more to the posterior border of the fenestra. The posterolateral process of the palatines is not preserved, so the extent of the palatines contribution to the lateral border is unclear. Wu and Chatterjee (1993) tentatively reconstructed the lateral process of the palatine as bordering the lateral edge of the fenestra, but we do not find evidence for this in the CT data.

4.1.2 | Bones of the cranium

Both of the **premaxillae** are nearly complete. There is a rugose region on the anterior end of the premaxilla that likely represents a break where the nasal process of premaxilla was located (Figures 3b, 4b,c, and 9b) and so the extent that the premaxilla contributed to the internarial bar is unknown. This region is similarly missing in *Dibothrosuchus* but has been preserved in *Dromicosuchus* (Sues et al., 2003), *Hesperosuchus* (CM 29894) (Clark et al., 2001) and *Sphenosuchus* (Walker, 1990) (Figures 3a and 9a). The anterior end of the right premaxilla has been pushed slightly toward the left, so that the narrow base of the broken internarial bar is a few millimeters left of the skull midline, and the facial portion of the left premaxilla has been displaced slightly medially where it contacts the maxilla. The premaxilla's contact with the maxilla is vertical and the entire posterior surface ventral to the posterodorsal process contacts the anterior surface

of the maxilla. In ventral view, the suture between the premaxilla and maxilla is straight. The preserved portion forms the ventral and posteroventral borders of the external nares, which faced anterolaterally (Figure 11c). The lateral surface posterior to the nares is approximately equal in length to the portion anterior to the posterior border of the nares when the posterodorsal processes are excluded from the total length. The shorter posterior process of the premaxilla is similar to some crocodyliforms, like *Fruitachampsa* (Clark, 2011) and *Dyrosaurus* (Jouve, 2005). Like other non-crocodyliform crocodylomorphs, the premaxilla bears a posterodorsal process that extends from the lateral surface between the anterior portions of the maxilla and nasal. The dorsal edge abuts the lateral edge of the nasal, which appears nearly flat in lateral view and the process extends posteriorly to above the level of the first preserved maxillary tooth. The dorsal edge of this process of the right premaxilla has a small indentation on its medial surface close to the narial border, but it is absent on the left side (Figure 9b). Assuming the internarial process was similar to other crocodylomorphs, the openings were narrow and elliptical in lateral view with the long axis running posterodorsally, which is also seen in *Dibothrosuchus*. The external surface of the lateral part immediately ventral to the narial opening has a shallow narial fossa, but a distinct border is lacking. There is only a very small subnarial gap (sensu Nesbitt, 2011) in the form of a slight ventral notch between the maxilla and premaxilla laterally where the fourth dentary tooth occludes (Figures 3b and 11a), unlike the far larger one seen in *Dibothrosuchus* and other non-crocodyliform crocodylomorphs such as *Sphenosuchus* (Walker, 1990), *Hesperosuchus* (CM 29894) (Clark et al., 2001), *Dromicosuchus* (Sues et al., 2003), and *Terrestrisuchus* (Crush, 1984) (Figure 10a) where the opening is large and constricted at its ventral edge. However, an internal pocket for enlarged dentary teeth is present, which is bordered anteriorly by the premaxilla and posteriorly by the maxilla notch (consistent with the subnarial foramen of Nesbitt, 2011), but is only visible in ventral view. The lack of a lateral notch is also seen in the non-crocodyliform crocodylomorph *Pseudhesperosuchus* (Bonaparte, 1969). The palatal portion of the premaxilla is short due to the anterior extent of the maxillary palatal process and does not meet medially, similar to other non-crocodyliform crocodylomorphs. A small, undivided incisive foramen is present on the midline where the maxilla and premaxilla meet opposite the posterior end of the narial opening. The ventrolateral edge of the premaxilla is gently convex ventrally, so that there is a gentle ventral concavity along the premaxillary symphysis and at the premaxilla–maxilla contact. Two faint circular impressions are preserved on the anterolateral surface of the premaxilla, dorsal to the third premaxillary tooth, which are interpreted as neurovascular foramina based on their small size and position dorsal to the toothrow.

The premaxilla of *Dibothrosuchus* is largely similar to that of *Junggarsuchus*; however, the two premaxillae of *Dibothrosuchus* are separate, likely due to postmortem deformation (Figures 5 and 10a). The premaxilla of *Dibothrosuchus* is taller, wider, and shorter than that of *Junggarsuchus* and the posterodorsal process of the premaxilla is shorter than that of *Junggarsuchus*, being less than half the length of the premaxilla anterior to the nares (Figures 5 and 10b). The nares face anterolaterally as in *Junggarsuchus*. On the anterior end of the premaxilla, anterior to the opening for the nares, there is a similar break to that of *Junggarsuchus*, which suggests the presence of the nasal process of the premaxilla though we cannot estimate its relative contribution to the internarial bar, a structure seen in other non-crocodyliform crocodylomorphs such as *Dromicosuchus* (Sues et al., 2003), *Hesperosuchus* (CM 29894) (Clark et al., 2001), and *Sphenosuchus* (Walker, 1990). The ventral edge of the premaxilla is in line with the ventral edge of the maxilla, unlike *Junggarsuchus*, in which the premaxilla's ventral edge is located dorsal to the majority of the maxilla's ventral edge. The palatal portion of the premaxilla is similarly short, but on the right premaxilla, a notch is present, medial to the fourth premaxillary tooth (Figure 11c); as it is not present in the left element, it is unclear whether this structure is asymmetrical or the result of post mortem deformation. Both elements also have a single small foramen on the anterior edge of the facial portion of the premaxilla, likely the same as that seen on *Junggarsuchus* (Figures 3a,b and 4a,b). *Dibothrosuchus* also possesses a slight depression on the facial portion of the premaxilla, but it is less concave than that in *Junggarsuchus*. Dorsal to the tooth row, the ventral most part of the lateral surface of the premaxilla has a slight ridge that trends along the entire length of the premaxilla and separates the tooth row from the rest of the lateral face. In *Dibothrosuchus*, this ridge is missing, and the bone dorsal to the tooth row is smooth. The greatest difference between the premaxilla of *Dibothrosuchus* and *Junggarsuchus* is the presence of the subnarial gap (Figure 3b), which occurs as a notch for the occlusion of the fourth dentary tooth. The notch between the premaxilla and maxilla in *Dibothrosuchus* is wide and ovate, nearly the length of the naris and more than half as wide (Figures 5 and 10a).

Each premaxilla of *Junggarsuchus* has five tooth positions, but the fifth tooth is preserved only on the right side. The anterior two right teeth were in the process of replacement as indicated by their small exposure relative to the teeth in the left premaxilla. Based on alveoli, which all occur as separate ventrally opening cavities, the

relative tooth sizes are 1 < 2 < 5 < 3 < 4. Only the posterior edge of the third, fourth, and fifth teeth is serrated. The anterior most two teeth are too poorly preserved to allow us to confidently describe any serrations. Serrations are similar in size to those of the maxillary teeth, each about 0.33 mm tall. The posterior third, fifth, and probably the fourth, teeth are slightly recurved, but are only slightly compressed labiolingually (Figures 3b, 4d, and 11b).

Dibothrosuchus has five teeth in its premaxilla, with relative sizes 1 < 2 < 5 < 3 < 4, just as observed in *Junggarsuchus*. None of the teeth are preserved in their entirety, and what teeth are observable lack serrations (Wu & Chatterjee, 1993). They have circular-ovate cross sections similar to *Junggarsuchus* teeth (Figures 5 and 11c).

Both **maxillae** are nearly complete, but both are missing a small portion just anterodorsal to the antorbital fenestra. The facial portion (Figures 3 and 4b) anterior to the antorbital fenestra is approximately 50% longer than it is tall in lateral view. Posteriorly, the maxilla divides into two processes that make up most of the dorsal and ventral borders of the antorbital fenestra. The posterodorsal process (=ascending process) meets the lacrimal approximately halfway along the dorsal edge of the antorbital fenestra; the suture between them is poorly preserved, but the lacrimal overlaps the maxilla laterally. The posterodorsal process is proportionally longer than those observed in other non-crocodyliform crocodylomorphs and appears to nearly totally separate the medial surface of the lacrimal from the lateral edge of the nasal. This posterodorsal process underlays the anterior edge of the lacrimal. The posterior process makes up the entire ventral border of the antorbital fenestra. The posteroventral process of the maxilla tapers gradually posteriorly, where the lacrimal broadly overlaps its posterior end. The tapered anterior end of the jugal inserts into the lateral surface of the posteroventral process of the maxilla to end dorsal to the last maxillary tooth and ventral to the center of the ventral edge of the lacrimal; the maxilla-jugal overlap extends for 10 mm. The premaxillary contact is extensive and nearly vertical anteriorly, and the anterior edge of the maxilla is slightly convex on the left side but not the right. The maxilla curves posterodorsally and is covered dorsally by the nasal along their straight contact in dorsal view. The ventral edge of the maxilla is gently convex at the positions of maxillary teeth three, four, and five and becomes straight posterior to the sixth tooth.

Anterior to the antorbital fenestra, the maxilla forms a very short fossa, preserved on the left side. On the dorsal edge of the fenestra, this fossa is dorsoventrally low forming a groove along the ventral edge of the maxilla's posterodorsal process. The fossa does not extend as far posteriorly or dorsally as that seen in *Dibothrosuchus*, *Dromicosuchus* (Sues et al., 2003), or *Hesperosuchus* (CM 29894) (Clark et al., 2001). Small ventrolaterally opening nutrient foramina pierce the ventrolateral surface of the maxilla dorsal to the tooth row, 12 on the right maxilla and 14 on the left (Figures 3a,b and 4b) and do not correlate one to one with the maxillary alveoli. The nutrient foramina are not evenly sized or space with the foramina more densely arranged dorsal to the third tooth. Along the medial surface of the posterodorsal process of the maxilla there is a groove, which continues onto the anteromedial surface of the lacrimal. We interpret this as for the maxillary branch of the trigeminal nerve (V2), as the passageway though the maxilla is dorsal to the alveoli, exhibits branching, and is in a similar position to the nerve observed in living crocodylians like *Alligator mississippiensis* (George & Holliday, 2013). The maxillary branch of the trigeminal nerve (V2) is preserved as a continuous passageway through the ventral body of the maxilla that extends the entire anteroposterior length of the bone. At least nine smaller ventral branches can be seen dorsal to the alveoli (Figure 6a,b). The spacing of these branches loosely follows the alveoli.

The two maxillae (Figure 5) of *Dibothrosuchus* are nearly complete and broadly similar to those of *Junggarsuchus*. Only the posterior most process that contacts the jugal is missing on the right maxilla. The maxillae are wider in articulation than those in *Junggarsuchus* and bow laterally posteriorly, though this lateral displacement is likely due to post mortem crushing (Figure 10). Unlike *Junggarsuchus*, the anterior end of the maxillae of *Dibothrosuchus* is concave in lateral view due to space for the enlarged fourth mandibular tooth that fits between the maxilla and premaxilla. The ventral edge of the maxilla is even more gently concave near the enlarged maxillary teeth than *Junggarsuchus*. The maxilla overlaps any lateral exposure of the nasal in latera view. The fossa also extends father posteriorly. Like *Junggarsuchus*, several ventrolaterally opening nutrient foramina pierce the ventrolateral surface of the maxilla. They are smaller and fewer than the ones present in *Junggarsuchus*, with eight to nine occurring dorsal to the tooth row. There also is an additional row of five or six small foramina on the dorsolateral surface of the posteroventral process of the maxilla immediately ventral to the ventral maxillary rim of the antorbital fenestra and dorsal to the posterior four neurovascular foramina (Figure 5). This row does not extend anterior to the anterior edge of the antorbital fenestra.

On the dorsal surface of both maxillae of *Dibothrosuchus*, there are two dorsal openings. The more anterior one (illustrated, but not described by Wu & Chatterjee, 1993), is located in line with the second maxillary tooth. The more posterior one is smaller and in line with the fourth maxillary

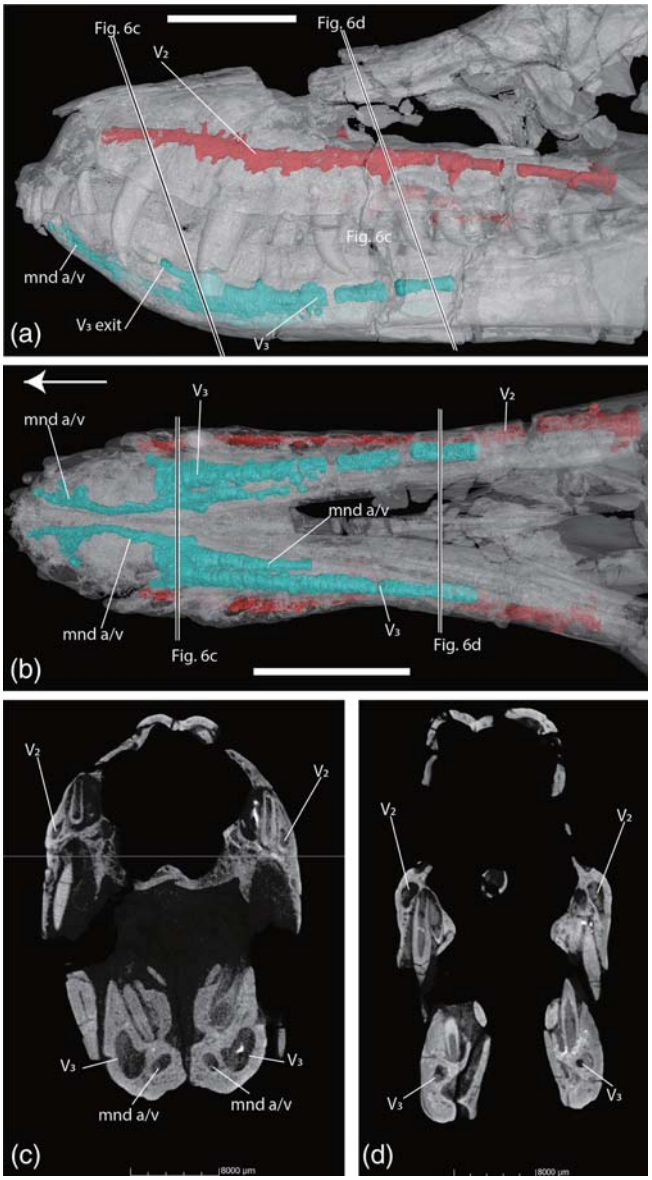

FIGURE 6 (a) The paths of the maxillary (red) and mandibular (blue) branches and associated vasculature of the trigeminal nerves in *Junggarsuchus sloani* in lateral view, figure made in VG studios; (b) the paths of the trigeminal nerves in ventral view; (c) cross sections of the maxilla and dentary in anterior CT view (slice 2,879); (d) cross section of the maxilla and dentary in CT view (slice 2,327). Black and white lines indicate where CT images in (c) and (d) were taken. Scale bar is equal 2 cm in (a)–(c) and 8 mm in (d) and (e). Arrow indicates anterior direction.

tooth. These openings are not seen in any other non-crocodyliform crocodylomorphs or crocodyliform. They appear to be due to postmortem crushing as they are associated with the roots of the tooth they correspond to (Figures 5 and 10). We interpret these as caused during deformation, as the dorsal surface of the skull was compressed, the roots of these teeth punctured the lateral wall of the maxilla, making weak spots.

The palatal process of the two maxillae in *Junggarsuchus* (Figure 11c) meets medially to form a bony palate. The bony palate begins anteriorly, between the premaxillae, and extends posteriorly up to the position of the fourth maxillary tooth. Anteriorly, the maxilla forms a pocket medial to the premaxillary contact into which the fourth dentary tooth inserted. This pocket opens dorsally, being visible from the narial opening. Posterior to this, the maxillary shelves of the palate become flatter in anteroposterior cross section and appear to thicken in CT scans, especially along the medial surface of the maxilla, where the two bones form a low midline ridge dorsally. The maxilla forms only the lateral and anterior borders of the choanae.

The palatal process of the maxilla of *Dibothrosuchus* (Figure 11e) is relatively wider than *Junggarsuchus*, though the partial separation is due to compression. The palatal shelf extends back to the position of the fifth maxillary tooth. A small medial extension of the palatal shelf forms the anterior and anterior most medial edges of the choanae. This process may be present in *Junggarsuchus*, but it is broken. However, there is a concavity on the ventral surface on the vomer that indicates its potential presence (Figure 11b).

We infer 14 tooth positions in each maxilla in *Junggarsuchus* (Figures 3b and 11b), the 14th is represented by an apparent tooth fragment in this position on the left side and alveolus on the right side. On both sides, the second and fourth teeth have been lost. The labial edge of the maxilla bulges laterally between the first and third teeth, indicating an alveolus, but the right maxillary edge extends inward at this position, possibly due to postmortem crushing. The third tooth is the largest and the alveolus for the fourth is smaller, whereas the first and fifth teeth are of similar size. The teeth gradually increased in size up to the third tooth, after which they decreased posteriorly. The third tooth is nearly twice as long as the fifth tooth, and the size of the alveoli and the ventral excursion of the maxilla in this region indicate that the second to fourth teeth were larger ones (the second tooth is nearly as anteroposteriorly long as the third and the fourth at least 25% longer based on the space of the alveoli) similar to the tooth positions in *Sphenosuchus* (Walker, 1990) and may have formed a functional unit separate from the posterior teeth. The fifth tooth is slightly smaller than the first tooth, and all teeth posterior to this become gradually smaller in size, until the last and smallest tooth is only 3 mm long. All of the teeth, except possibly the posterior one, are recurved, and the sixth and seventh are strongly recurved. The distal edge of each maxillary tooth is serrated in a similar manner

(Figure 4d). The mesial edge is also serrated on its distal half from the sixth tooth posteriorly, but the first and third teeth lack serrations mesially. A small, loose tooth is preserved on the lateral surface of the right dentary beneath the posterior end of the tooth row, similar in size to the 13th preserved maxillary tooth, and therefore it is possibly the 14th tooth.

Dibothrosuchus has positions for 15 maxillary teeth on both sides (Figures 5 and 11c). On the left side only alveoli 8, 10, and 15 are empty, and on the right side only alveoli 4, 14, and 15 are empty. The first two maxillary teeth are small, the second slightly larger than the first, but both are barely exposed laterally. The largest teeth and alveoli are the third and fourth teeth. Both the fourth alveolus and tooth are slightly larger, but neither the third or fourth tooth are preserved entirely, those seen are missing the apical ends of the crown. The fifth tooth is smaller than the third and fourth, but larger than the others. Relative to the height of the maxilla, the enlarged maxillary teeth (crowns at least 30% the height of the maxilla) are not as large as those of *Junggarsuchus*, which has enlarged maxillary tooth crowns at least 60% the total height of the maxilla. Like *Junggarsuchus*, the rest of the teeth decrease in size posterior to the 14th tooth. The maxillary teeth of *Dibothrosuchus* are recurved but slightly less recurved distally than those of *Junggarsuchus*. The seventh tooth is the most recurved. Like *Junggarsuchus*, the lanceolate hypertrophied maxillary teeth lack anterior serrations and from the sixth tooth posteriorly are serrated distally and mesially.

The **nasals** of *Junggarsuchus* are paired, long, narrow bones that make up the anterior half of the skull roof anterior to the orbit. They widen posteriorly in the lateral direction and reach their widest point at about 75% of their length, near their contact with the prefrontals, then narrow where it meets the frontal (though remain twice the width of the anterior part of the nasals) similar to *Sphenosuchus* (Walker, 1990), the crocodyliform *Orthosuchus* (Nash, 1975), and thalattosuchians like *Pelagosaurus* (Pierce & Benton, 2006) (Figure 9b). This differs from the condition in *Protosuchus richardsoni* (MCZ 6727, AMNH 3024, and UCMP 130860) (Clark, 1986) in which the nasals widen posteriorly to a transverse contact with the frontals. A large, central area where the nasal would have contacted the maxilla on both the right and left sides is missing, and the left nasal is also damaged anterior to this gap. Anterior to the prefrontal, their lateral edge bends ventrally, dividing the bone into dorsally and laterally facing parts. The dorsal part is slightly convex dorsally in the anterior half of the bone, resulting in a dorsal midline groove. Posteriorly, the nasals are nearly flat and rise medially to form a low midline ridge. The anterior ends of the nasals form a small part of the posterodorsal border of the external nares, which fit between both premaxillae. The nasal contacts the posterodorsal process of the premaxilla ventrolaterally and the nasal widens slightly anterior to this process. The nasal ends anteriorly in a broken base of the internarial process, which is broad and dorsoventrally flattened (Figures 3a, 5c, and 9a,e). The posterior end of the nasal does not feature a w-shaped suture with the frontals (Figure 9b). Two lateral posterior processes on the nasal extend between the prefrontal and frontal, where it overlies, the frontal and prefrontal partially. These posterior processes are similar to those in *Dibothrosuchus* and *Hesperosuchus* (CM 29894) (Clark et al., 2001), but the portions of the bone extending between the prefrontals and frontal are much shorter (about one-tenth the anteroposterior length of the prefrontal vs. one-third the length in *Dibothrosuchus*). Anterior to the prefrontal, the nasal has a short contact laterally with the anterodorsal process of the lacrimal. Unlike other non-crocodyliform crocodylomorphs, the lateral edge of the nasal does not contact the medial edge of the maxilla instead, the ventrolateral surfaces of the nasals contact the dorsal surface of the posterodorsal (=ascending) process of the maxilla. Posteriorly, the lateral edges of the nasals are largely excluded from contacting the medial edge of the lacrimal by the prefrontals. This is similar to the conditions seen in *Protosuchus haughtoni* (BP/1/4770) and *Orthosuchus* (Nash, 1975).

The paired nasals of *Dibothrosuchus* are more complete (Figure 10), with the exception of the anterior ends that extends between the premaxilla that would meet the internarial bar (Figure 10c). The nasals have been displaced ventrally, due to post mortem distortion. The nasal is largely similar to that of *Junggarsuchus*; it contacts the dorsal edge of the maxilla along its anterior third, and contacts the medial edges of the prefrontals posteriorly. There is also a short, 4-mm-long contact with the medial edge of the lacrimals posteriorly. Unlike the nasals of *Junggarsuchus*, the nasals of *Dibothrosuchus* do not widen posteriorly, and overall, are relatively wider than those of *Junggarsuchus*. The two bones are flatter, lacking the slight dorsal ridges present in other non-crocodyliform crocodylomorphs. The nasals also lack the lateral exposure seen in *Junggarsuchus* and possess a more distinct forked process of the posterior part of the nasals, which extend between the prefrontals and the frontals. These twinned posterior processes are separated by an anterior process of the frontals at the midline and are wider than those seen in *Junggarsuchus*.

The **lacrimal** of *Junggarsuchus* is in the shape of an inverted L with a long anterodorsal process and is approximately as long as it is high (Figures 3b and 9b). On the right side of the skull, the bone has been partially

crushed, and the left element is better preserved. Its ventral process is nearly vertical in lateral view, forming the posterior edge of the antorbital fenestra. The anterior edge of this process has a deep dorsoventral groove (Figures 3b and 7b) that becomes open laterally near the base, forming a narrow antorbital fossa. The posterior edge of this process curves posteroventrally, forming the anteroventral edge of the orbit, and is as long as the ventral process of the lacrimal at its midpoint. This elongate posteroventral process is longer than the process seen in *Dibothrosuchus*, which is only 50% of the length of the lacrimal's ventral process at its midpoint. The lacrimal has a very narrow exposure on the skull roof and contacts the prefrontal medially and posteriorly dorsal to the preorbital bar. The posterior contact with the prefrontal is short, and the prefrontal dorsally covers the posterior edge of the entire dorsal part of the lacrimal. The tapering anterodorsal process overlies the maxilla approximately at the midpoint of the antorbital fenestra, but this suture has been damaged on both sides of the skull. The dorsal part of the lacrimal has a rugose lateral surface, whereas the descending process has a smooth surface. Medially, within the skull, a large but shallow pocket is visible on the medial surface of the anterodorsal body of the lacrimal (Figure 7b). Based on its position well anterior to the orbit and the ventral lamina (=cristae cranii sensu Walker, 1990) of the frontal, we infer this as an excavation of the paranasal sinus; a similar pocket is present in *Dibothrosuchus*. The mediolateral wall of the lacrimal body is relatively thin and the anterior surface of the ventral process preserves a narrow dorsoventral groove that forms the posterior border of the antorbital fenestra, and we infer the lip of it to be the posterior limit of the antorbital sinus. There is an elongate, continuous space through the anterodorsal body of the lacrimal for the nasolacrimal duct, that is circular in cross section and nearly, but does not fully reach the anterior border of the antorbital fenestra. The anterior end of the duct opens medially into the skull at the end of the anterodorsal process of the lacrimal and the duct opens posteriorly into the orbit though an oval foramen, the lacrimal foramen (Figure 7d,e). This posterior exit into the orbit is set in a rhomboidal depression enclosed anteriorly by the lacrimal and posteriorly by the prefrontal (Figure 7a). The passageway is horizontal for much of its length. In lateral view, the passageway expands dorsally three-fourths of the way back, near the tallest point of antorbital fenestra. The passageway for the nasolacrimal duct then descends ventrally for the remainder of its length.

The lacrimal of *Dibothrosuchus* is similar to that of *Junggarsuchus* (Figures 5 and 7c). The anterodorsal process of the lacrimal is about the same length as the ventral process, which is proportionally longer than the process in *Junggarsuchus*, and forms the posterior half of the dorsal border of the antorbital fenestra. The lacrimal is longer than the prefrontal anteroposteriorly, which is similar to the relative length of the lacrimal to the prefrontal seen in *Protosuchus richardsoni* (AMNH 3027, UCMP 130860), *Protosuchus haughtoni* (BP/1/4770) (Gow, 2000) and other early diverging crocodyliforms like *Orthosuchus* (Nash, 1975), *Gobiosuchus* (Osmólska et al., 1997), and most Thalattosuchians, but not *Junggarsuchus* or *Sphenosuchus* (Walker, 1990). The groove that extends into the anterior antorbital fossa is shorter in *Dibothrosuchus*. The lacrimal appears to lack the posterior projection that overlays the anterior portion of the prefrontal, but the bone is crushed in this region on both sides, obscuring potential sutures. In *Dibothrosuchus*, the contact with the prefrontal extends ventrally for most of the lacrimal's ventral process, and the suture is vertical. As in *Junggarsuchus*, the lacrimal is thin walled and possesses an enlarged hollow space in the anterior body of the bone, relatively larger than that of *Junggarsuchus*. The posterolateral surface of the lacrimal, along the dorsoventral suture with the prefrontal, has a small opening for a lacrimal foramen that opens into the orbit, which is enclosed by the lacrimal laterally and the prefrontal medially (Figure 7c). In *Junggarsuchus*, the posterior exit of the nasolacrimal duct is set in a lateral depression between the lacrimal and prefrontal, whereas the actual posterior exit of the duct is fully enclosed in the lacrimal, contrasting with the condition in *Dibothrosuchus* (Figure 7a,b).

The rhomboidal **prefrontal** of *Junggarsuchus* overhangs the orbit anteriorly (Figures 3b, 8b, and 9b). Its mediolaterally broad ventral process extends into the anterodorsal region of the orbit, where its anteroposteriorly long and triangular lateral part borders the lacrimal posteriorly. This process forms the anterodorsal half of the orbit and medially it curves posteriorly to form a posterolaterally facing fossa. The body of the laterally expanded prefrontal makes up the anterior half of the orbit's dorsal border. The medial part of the descending process is mediolaterally thinner than the lateral part, its ventral edge is horizontal and its posterior edge is vertical (Figures 3b and 8b). Anterodorsally, the prefrontal narrows and fits between the lacrimal and the nasal. The contact with the frontal is approximately as long as the contact with the nasal. Posteriorly, as in *Dibothrosuchus*, the prefrontal does not appear to send a mediolaterally wide process to underlie the frontal, contrasting with the condition reported in *Sphenosuchus* (Walker, 1990) and *Hesperosuchus* (CM 29894) (Clark et al., 2001), though this is challenging to verify without CT data for these taxa. Its dorsal surface is shallowly concave posteriorly and becomes slightly convex in the area where it contacts the lacrimal. *Junggarsuchus* has a laterally expanded

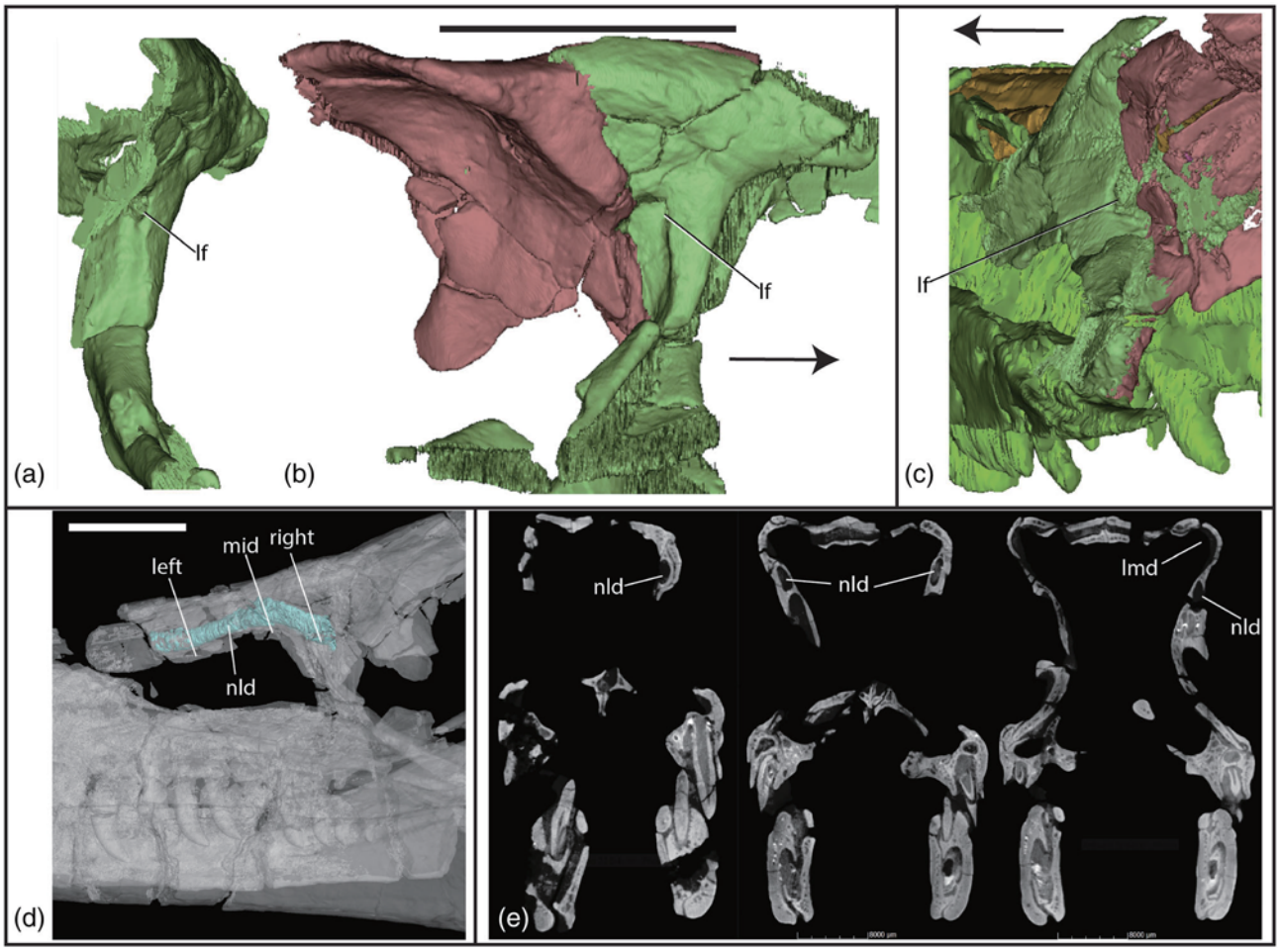

FIGURE 7 (a) The lacrimals of *Junggarsuchus sloani* in posterolateral view; (b) left lacrimal and prefrontal of *Junggarsuchus sloani* in lateral view showing rhomboidal depression for the lacrimal foramen; (c) the lacrimals of *Dibothrosuchus elaphros* in posterolateral view; (d) endocast of the nasolacrimal duct in lateral view; (e) nasolacrimal duct in cross section in CT view—anterior exit (left—slice 2,199), middle (slice 1,921), and posterior exit (right—slice 1,834). Black and white lines indicate where CT images in (e) were taken. Scale bars are equal to 2 cm in all figures except (e) where the scale bar equals 8 mm. Arrow indicates anterior direction.

prefrontal which forms a prefrontal overhang on the anterodorsal half of the orbit which is not observed in *Dibothrosuchus*, *Sphenosuchus* or other non-crocodyliform crocodylomorphs. The overhang is enlarged, twice the mediolateral width of the anterior process, and oblique, similar to the overhang seen in thalattosuchians such as *Pelagosaurus*, though not as enlarged as those overhangs in metriorhynchids like *Cricosaurus* ("*Geosaurus*") *araucanensis* (Young & Andrade, 2009), *Dakosaurus maximus* (Young et al., 2012) and *Metriorhynchus* (Andrews, 1913). The posterior face of the orbital fossa of the prefrontal has a small foramen that is directed posteriorly (Figure 8a, b). This foramen is preserved on both prefrontals and is likely an opening for the anterior path of the supraorbital vein or artery, because in extant crocodylians, the supraorbital vein passes through the frontals, exits the frontal and rests along the dorsomedial border of the orbit, then reenters the skull through the posterior surface of the prefrontal where it then continues into the nasal capsule (Porter et al., 2016). This foramen in the posterior face of the prefrontal is consistent with this interpretation, though the path of this vein through the frontal is not preserved and it is possible that the vein was resting on the exterior of the frontal in the orbit, then entering the skull and nasal capsule through the prefrontal. In living crocodilians, the supraorbital veins and arteries are closely associated with the ophthalmic branch of the trigeminal nerve, and this path of the trigeminal nerve is positioned medial to the prefrontal and does not enter the bone so it is unlikely that this foramen is for the ophthalmic branch of the trigeminal (Lessner & Holliday, 2020).

The prefrontal of *Dibothrosuchus* (Figures 5 and 10a) is largely similar to that seen in *Junggarsuchus* in being rhomboidal in dorsal view. More of the descending medial and posterior processes of the prefrontal are preserved in *Dibothrosuchus*. Like *Junggarsuchus* and other non-crocodyliform crocodylomorphs, the prefrontal of

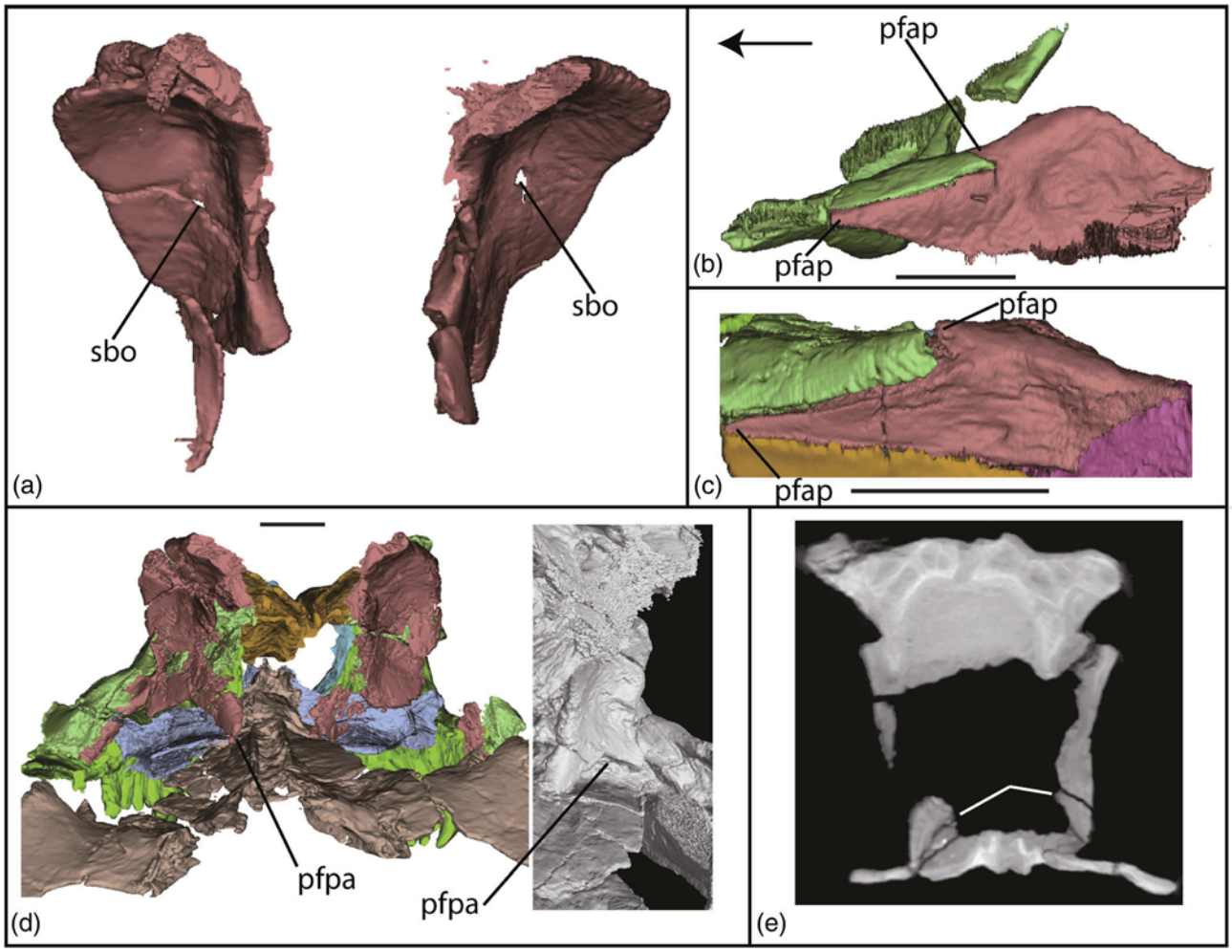

FIGURE 8 The prefrontals of *Junggarsuchus sloani* in (a) posterior and (b) dorsal views; prefrontals of *Dibothrosuchus elaphros* in (c) dorsal view, and (d) the prefrontals and palate in posterior view visualized in mimics (left) and as an isosurface render (right); (e) lack of prefrontal brace seen in CT data, indicated by white line (slice 1,541). Arrow indicates anterior direction; scale bars are 1 cm.

Dibothrosuchus features a concavity for the posterior process of the lacrimal along with forked anterior processes of the prefrontal; the additional lateral process is partially broken anteriorly (Figures 5 and 10a). The anterodorsal process of the prefrontal is longer and has a longer contact with the nasal than it does in *Junggarsuchus*. The posterior dorsal suture of the prefrontal with the frontal is not very clear, but it appears that not much of the prefrontal extends under the frontals. As in *Junggarsuchus*, the dorsal surface is concave medially and convex and ridge like laterally, though this may have been exaggerated by crushing. *Dibothrosuchus* lacks a prefrontal overhang.

The descending process of the prefrontal in *Dibothrosuchus* (Figure 5) extends farther ventrally and posteriorly than the process in *Junggarsuchus* and forms the entire anteromedial wall of the orbit. This is a greater contribution to the orbital wall than observed in any other non-crocodyliform crocodylomorphs, including *Sphenosuchus* (Walker, 1990). The medial contact of the prefrontals to form a "transverse-brace" reported by Wu and Chatterjee (1993) is not observed in the CT scans of the skull (Figure 7d,e). The ventral process of the prefrontals that contact the palatines do not appear to contact each other and, based on inferences from CT, data do not appear the medial surface of these ventral processes are broken (Figure 8c,d). The descending process contacts the palate at the point that the posterior edges of the palatine and meet lateral edges of the pterygoid. The contact between the prefrontal and palate is not observed in any other non-crocodyliform crocodylomorphs, but it is present in crocodyliforms including *Gobiosuchus* (Osmólska et al., 1997) and the more specialized thalattosuchians (*Cricosaurus* and *Metriorhynchus*) (Young & Andrade, 2009) and notosuchians and neosuchians. Despite the dorsoventrally tall ventral processes of the prefrontal, this contact may, however, be due

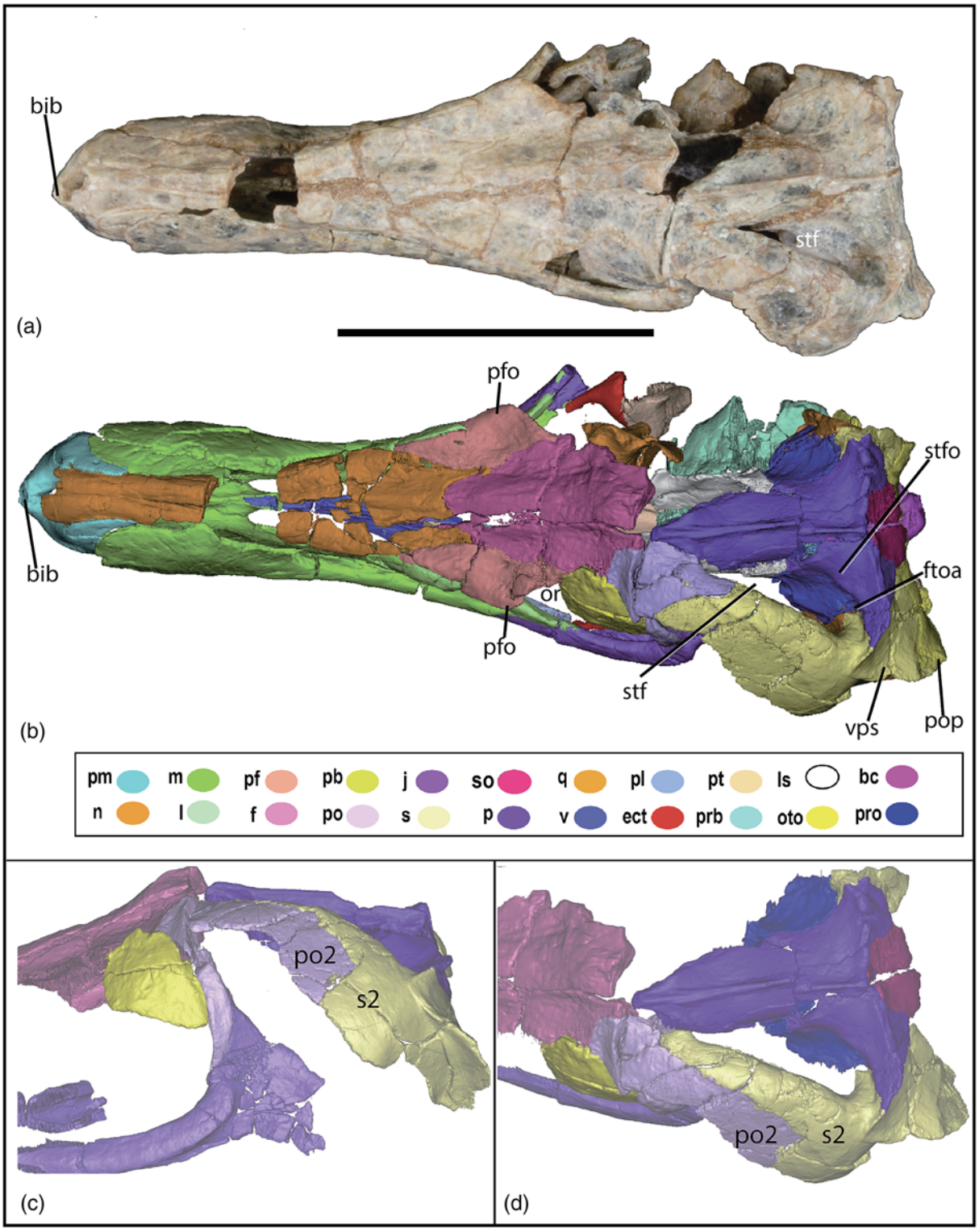

FIGURE 9 Photograph of the skull of (a), *Junggarsuchus sloani*; (b) CT reconstruction of the skull of *Junggarsuchus sloani* in dorsal view; (c) alternative interpretation of the postorbtial, frontal, squamosal contact in *Junggarsuchus sloani* in dorsal view; (d) alternative interpretations of squamosal–postorbital contact in *Junggarsuchus sloani* in left lateral view. Scale bar is equal to 5 cm.

to dorsoventral crushing of the skull. Unlike neosuchians, in which the ventral processes of the prefrontal's are expanded laterally and medially and widely contact the palatines, *Dibothrosuchus* lacks the ventral expansion of the ventral processes of the prefrontal which would not have provided the support it does in neosuchians.

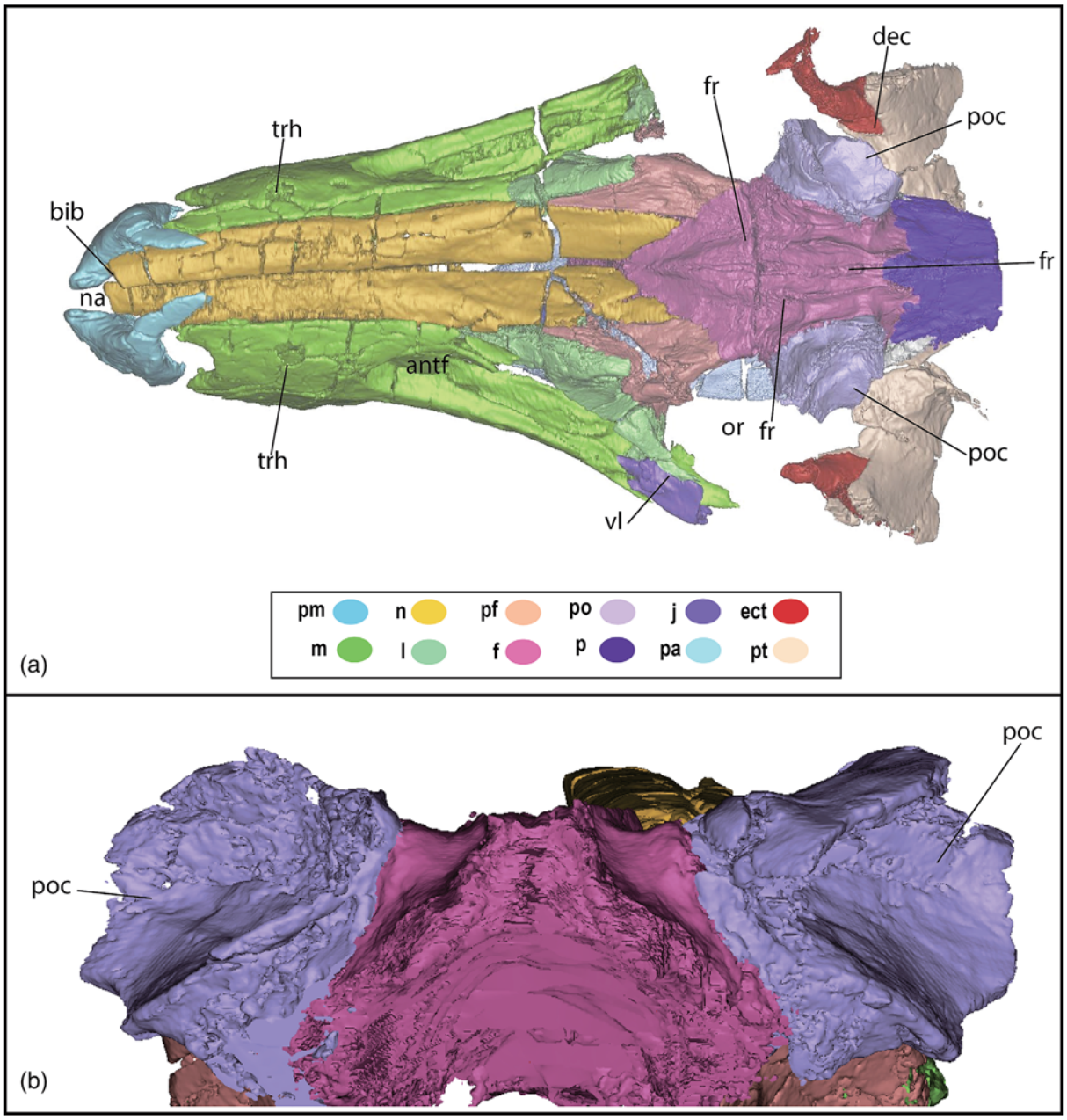

FIGURE 10 (a) The rostrum and orbital region of *Dibothrosuchus elaphros* in dorsal view; (b) postorbitals in posterior view; scale bars are equal to 1 cm.

In *Junggarsuchus*, the paired **frontals** form the skull roof medial to the orbits, posterior to the nasals and prefrontal, and anterior to the parietal and postorbital (Figures 3b and 9b). The frontal forms the posterodorsal margin of the orbit. The orbital margin is only preserved on the left side, where the palpebral covers it, and the frontal appears to be laterally concave. However, this concavity may be accentuated by the palpebral, which has been pressed unnaturally onto the surface of the frontal. Inside the orbit, the crista cranii (sensu Walker, 1990), forming the lateral margin of the olfactory tract, is mediolaterally thin but extends ventrally much further than in living crocodylians (Figures 3b and 4b). The crista is incomplete, but its anterior end is preserved on both sides where it contacts the medial surface of the descending process of the prefrontal. Posteriorly, a fragment of the left crista is preserved on the lateral surface of the braincase. A broad, low longitudinal ridge, similar to that of *Sphenosuchus* (Walker, 1990) and *Hesperosuchus* (CM 29894) (Clark et al., 2001), trends along the central region of the dorsal surface of the frontals the entire length. Anteriorly, the frontals form a blunt process at the midline that wedges between the posterolateral processes of the nasals. A thin, ventrally offset projection of

the frontals anterior to the frontal–nasal contact is overlain by the nasals on the midline.

Anterolaterally, the frontal contacts the posterior part of the prefrontal along a posterolaterally trending oblique suture. The frontals have a posterolaterally concave contact with the dorsal part of the postorbital in dorsal view. The posterior ends of the frontals are broken, corresponding to a large fracture in the specimen, the posterior end of the frontal does not extend as far laterally as in *Hesperosuchus* (CM 29894) (Clark et al., 2001), *Sphenosuchus* (Walker, 1990) and *Protosuchus richardsoni* (AMNH 3024, UCMP 130860, MCZ 6727) (Clark, 1986), giving the supratemporal fenestra its triangular rather than oval shape.

The paired frontals of *Dibothrosuchus* are similar in position to other non-crocodyliform crocodylomorphs (Figures 5 and 10a). However, the frontal lacks the deep lateral concavity seen in *Junggarsuchus*. The concavity is far shallower, which may be related to the lack of a palpebral. The cristae cranii of *Dibothrosuchus* are dorsoventrally shallower than observed in *Junggarsuchus*, though they may be broken. The frontal is also proportionally wider laterally, giving the supratemporal fenestra a more oval shape, but lacks the posterolateral processes seen in *Sphenosuchus* (Walker, 1990). The parasagittal ridges on the dorsal surface of the skull are dorsoventrally taller in *Dibothrosuchus* than they are in *Junggarsuchus*, which has lower dorsal ridges. The median ridge of the frontal is divided by a wide groove along the midline resulting in two midline ridges around the central ridge along the suture. These ridges converge anteriorly and posteriorly into a lanceolate shape (Wu & Chatterjee, 1993). Posteriorly, the parasagittal ridges are laterally separated from the postorbitals by another deep groove and ridge along the suture. This is a feature unique to *Dibothrosuchus* (Wu & Chatterjee, 1993). Anteriorly, the frontals narrow and have an anterolateral contact with the posteromedial edges of the nasals that is about 25% of the total length of the frontals. In *Dibothrosuchus*, this anterior narrowing is triangular, unlike the rounded anterior edge seen in *Junggarsuchus* (Figures 9b and 10a).

The left **palpebral** is observed only in *Junggarsuchus* and is preserved in contact with the frontal and postorbital bones at the dorsal margin of the left orbit, its lateral edge is displaced slightly ventromedially from its presumed sub-horizontal position (Figures 3b and 9b). It is ovoid in dorsal view, with an anteromedial–posterolateral long axis that divides the bone nearly symmetrically. It is dorsally convex and its surface is covered with a low, rugose sculpturing. Its posterior edge is preserved contacting the anterior edge of the postorbital and roughly reflects the latter's shape. This edge is only gently curved, less so than other edges. The posterolateral and anteromedial edges of the bones are acutely angled, roughly 72° (Figures 3b and 9b). The medial part of the bone, which overlies the frontal, has a small notch. In the only other non-crocodyliform crocodylomorphs for which a palpebral is known, *Hesperosuchus agilis* (CM 29894), it is more circular in shape, dorsoventrally thicker, and has very fine, extensive sculpturing.

The anterior process of the triradiate **jugal** in *Junggarsuchus* inserts into the posterior end of the maxilla, where the ventral process of the lacrimal borders it dorsally (Figures 3a,b and 4a,b). Posteriorly, the jugal widens mediolaterally, where it forms the ventral border of the orbit; this region is marked by a concave longitudinal depression along its entire ventrolateral surface. The bone then curves posterodorsally to form the posteroventral border of the orbit and the ventral half of the postorbital bar. Thus, its ventral edge is not flat, as in other non-crocodyliform crocodylomorphs like *Dibothrosuchus* and in many crocodyliforms like *Orthosuchus* (Nash, 1975), *Fruitachampsa* (Clark, 2011), *Gobiosuchus* (Osmólska et al., 1997), *Hsisosuchus* (Li et al., 1994), and neosuchians like *Crocodylus niloticus*. Instead, it is ventrally concave ventral to the postorbital bar, opposite the dorsal convexity of the surangular. The medial surface ventral to the orbit also possesses a longitudinal groove, bordered ventrally by a horizontal ridge along the ventral part of the bone (Figure 11c). The dorsal process of the jugal is covered by the descending process of the postorbital medial to the postorbital unlike other non-crocodyliform crocodylomorphs and most crocodyliforms, but as in thalattosuchians like *Cricosaurus* ("*Geosaurus*") *araucanensis* (Young & Andrade, 2009).

Posterior to the postorbital bar, the concavity on the ventrolateral surface of the jugal opens into a broad, thin, medially depressed lower temporal bar (Figure 3b). It is not clear which part of this region is formed by the jugal and which by the quadratojugal due to numerous breaks in the region of the lower temporal fenestra. The jugal most likely continues posterior to its contact with the postorbital (the jugal process contributing to the postorbital bar extends to about the midpoint of the ventral process of the postorbital), where there is a distinct suture, but this could also be the quadratojugal, as in some non-crocodyliform crocodylomorphs (Clark et al., 2001). The dorsal extent of the posterior process appears to nearly reach the posterior edge of the lateral temporal fenestra, whereas the posteroventral process extends further, possibly to the posterior end of the quadratojugal. The quadratojugal appears not to extend that far anteriorly, as discussed below, and the anterior half of the lower temporal bar is formed mostly by jugal. The posterior process of the jugal slopes posteroventrally posterior to the postorbital bar and is slightly shorter than the anterior process, unlike other non-crocodyliform crocodylomorphs

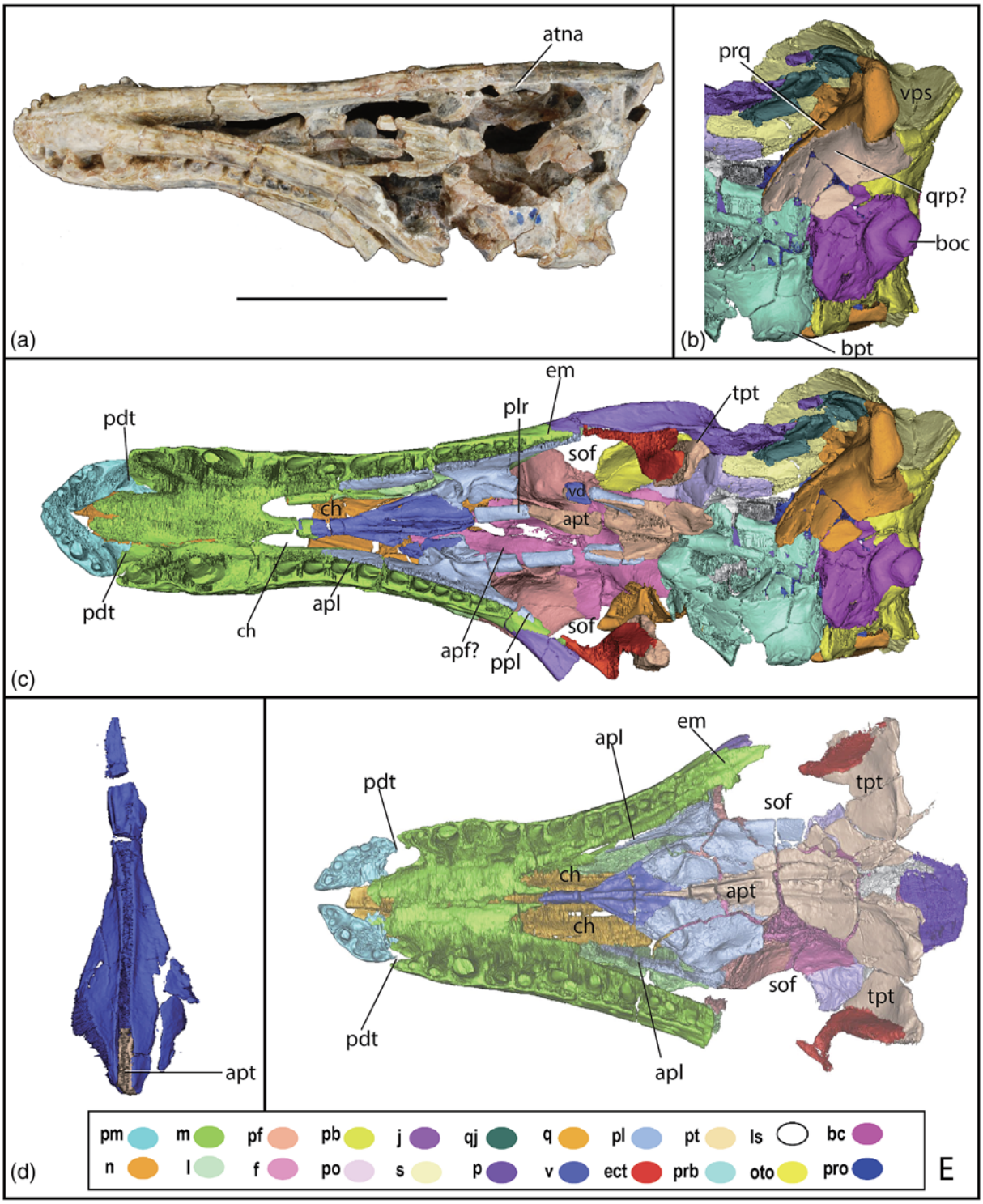

FIGURE 11 Photograph of the skull of (a) *Junggarsuchus sloani* in ventral view; (b) alternate CT reconstruction of the quadrate and pterygoid in *Junggarsuchus sloani* in ventral view; (c) CT reconstruction of the palate of *Junggarsuchus sloani* in ventral view; (d) vomer of *Junggarsuchus sloani* in dorsal view, anterior tip at the top of the image; (e) CT reconstruction of the rostrum and orbital region of *Dibothrosuchus elaphros*, in ventral view. Scale bar is equal to 5 cm in (a) and 1 cm in (e).

(Walker, 1990; Wu & Chatterjee, 1993). Posteroventral to the main body of the jugal and anterior to the quadratojugal an isolated broken oval section of bone is present which we reconstruct as jugal based on its position, which appears continuous with the rest of the jugal (Figure 3b). There is possibly an anteroposteriorly long contact between the jugal and quadratojugal, like the contact seen in early diverging crocodyliforms like

Protosuchus haughtoni (BP/1/4770) (Gow, 2000), *Protosuchus richarsoni* (AMNH 3024, UCMP 130860) (Clark, 1986), and *Zaraasuchus* (Pol and Norell 2004a) that reduces the size of the infratemporal fenestra. The lower temporal bar is dorsoventrally tall, nearly 50% of the height of the orbit, compared to *Sphenosuchus* (Walker, 1990) and is very thin mediolaterally.

Only the anterior end of the left jugal is known from *Dibothrosuchus* IVPP V 7907 (Figure 5b). The jugal is better known from CUP 2981 (Simmons, 1965), which allows for comparison to *Junggarsuchus*. The anterior tip of the jugal has two anterior processes, and the anterodorsal tip just barely participates in the posterior border of the antorbital fenestra (Figure 5). The jugal narrows in its dorsoventral height posteriorly, unlike *Junggarsuchus*. The posterior process of the jugal of *Dibothrosuchus* is straight, unlike *Junggarsuchus*, like most other early diverging crocodylomorphs and is not dorsally arched. The dorsal process of the jugal that contacts the postorbital bar lies lateral to the postorbital, as in most crocodyliforms like *Protosuchus richardsoni* (AMNH 3024) (Brown, 1933; Clark, 1986) and *Crocodylus niloticus*.

The **parietal** in *Junggarsuchus* lacks any trace of a midline suture, unlike in some non-crocodyliform crocodylomorphs such as *Litargosuchus* (Clark & Sues, 2002), *Hesperosuchus* (CM 29894) (Clark et al., 2001) and *Dromicosuchus* (Sues et al., 2003) (Figures 3b and 9b; Leardi et al., 2017). The parietal bears a sharp T-shaped crest in dorsal view that is comprised of an anteroposteriorly trending, mediolaterally narrow sagittal crest that trends along the entire midline length of the parietal and the nuchal (supraoccipital) crest that runs mediolaterally along the entire occipital portion of the skull roof. Anteriorly, the sagittal crest continues onto the posterior end of the frontals where it expands mediolaterally to twice the width of the crest at its posterior end, but the contact between the frontal and parietal is obscured by a large crack. In dorsal view, the crest along the posterior margin of the parietal is set at a 90° angle from the sagittal crest, as opposed to the V-shaped crest seen in almost all other non-crocodyliform crocodylomorphs except *Dibothrosuchus*, *Sphenosuchus* (Walker, 1990), and *Almadasuchus* (Clark, Xu, Forster, & Wang, 2004; Pol et al., 2013). The sagittal crest continues into a dorsal occipital (nuchal) crest laterally and curves anterolaterally at the posterolateral portion of the supratemporal fossa, and then continues onto the posterodorsal surface of the squamosal. The lateral edge of the body of the parietal is dorsolaterally convex and forms the medial and posteromedial border of the supratemporal fenestra. The parietal meets the squamosal in an anteromedially oblique suture approximately midway around the posterior edge of the fenestra. A small anterior opening to the anterior temporal foramen (Figure 9b) is situated between the parietal and squamosal, and the parietal forms the medial and dorsal edges of the foramen, whereas the prootic forms the ventral edge. The posterodorsal part of the supratemporal fenestra faces anterodorsally and forms only a short fossa rather than the much anteroposteriorly longer ones that often floors up to 50% of the supratemporal fenestra in early diverging crocodyliforms like *Orthosuchus* (Nash, 1975), ziphosuchians like *Baurusuchus salgadoensis* (Nascimento & Zaher, 2010), living crocodylians, *Dibothrosuchus*, *Almadasuchus*, and *Pelagosaurus* (Pierce & Benton, 2006). The parietal has a small process that fits onto the occipital surface and is rhomboidal in posterior view, overlaying the dorsal edge of the supraoccipital as in *Dibothosuchus* (Figure 12). The parietal also extends onto the occipital surface between the supraoccipital and squamosal and rests on the paroccipital process (Figure 13). It forms the dorsal border of the posttemporal fenestra, like in *Sphenosuchus* (Walker, 1990). The occipital portion of the parietal is triangular in occipital view, with a low, gently convex ventral end, and a broad dorsal base. The posterolateral process of the parietal extends dorsolaterally as a slender process over the squamosal to reach the posterodorsal corner of the supratemporal fossa and posterior skull roof. In *Dibothrosuchus* and crocodyliforms like *Protosuchus richardsoni* (MCZ 6727, AMNH 3024, and UCMP 130860), this posterolateral process is shorter and does not reach the posterolateral corner of the supratemporal fenestra. The dorsal roof of the braincase is formed by the parietals. Although the parietals contact with the frontals is not well preserved in *Junggarsuchus* due to a break, it appears that a small portion of the parietal projects between the posterior extension of the frontal and the laterosphenoid. This is similar to the condition seen in some thalattosuchians like *Steneosaurus bollensis*, *Pelagosaurus typus* (Pierce & Benton, 2006) and *Cricosaurus* ("*Geosaurus*") *araucanensis* (Young & Andrade, 2009), though the process is not elongate and does not participate in the supratemporal fossa.

The parietals of *Dibothrosuchus* (Figures 5, 10a, and 25a,d) have a lower sagittal crest than *Junggarsuchus* that is T-shaped in dorsal view, and features a visible midline suture anteriorly, though it is only visible due to a break in the sagittal crest. The parietals anterior contacts with the frontals are blunt and rectangular, though there is a slight anteromedial process that projects anteriorly. The lateral expansions of the occipital ridge do not extend as far laterally as those of *Junggarsuchus* and contribute to less than half of the medial posterior border of the supratemporal fenestra. The posttemporal fenestra is much larger in *Dibothrosuchus*, similar to *Sphenosuchus* (Walker, 1990) rather than *Junggarsuchus*. The parietal does not contribute to the edges of the anterior temporal foramen in *Dibothrosuchus*, where the medial and ventral

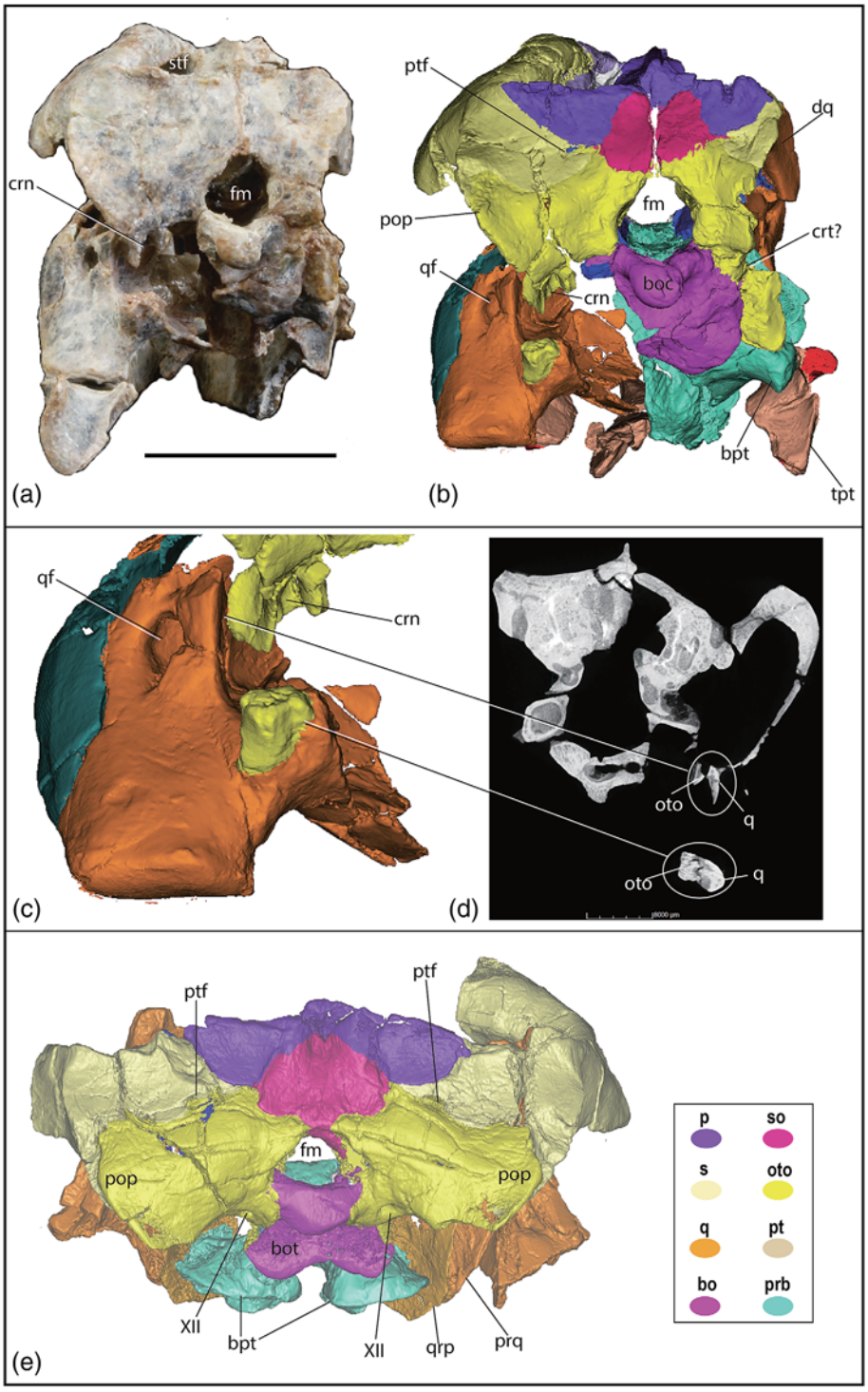

FIGURE 12 Occipital view of the skull of *Junggarsuchus sloani* in (a) a photograph and (b) CT reconstruction; (c) left quadrate otoccipital contacts; (d) CT cross section of quadrate occipital contact (slice 369); (e) CT reconstruction of the skull of *Dibothrosuchus elaphros* in occipital view. Scale bar is equal to 3 cm in (a) and 1 cm in (e).

edge are formed by the prootic and the dorsal edge by the squamosal (Figure 25b). The parietal and prootic contribute to a broader supratemporal fossa than seen in *Junggarsuchus*. The parietal of *Dibothrosuchus* is involved in the occipital portion of the skull, which has a medial rhomboidal projection into the supraoccipital and expanded rectangular processes that separate the squamosal and supraoccipital in occipital view. Unlike *Junggarsuchus*, the parietals of *Dibothrosuchus* do not contribute to the medial or dorsal edge of the fenestra. The parietals end dorsal to a thin process of the squamosal that forms the border of the posttemporal fenestra. *Dibothrosuchus* shares this parietal involvement in the posttemporal fenestra with other early diverging non-crocodyliform crocodylomorphs.

The ventral process of the **postorbital** in *Junggarsuchus* makes up the dorsal half of the postorbital bar and has a broad dorsal portion (Figure 3b). The

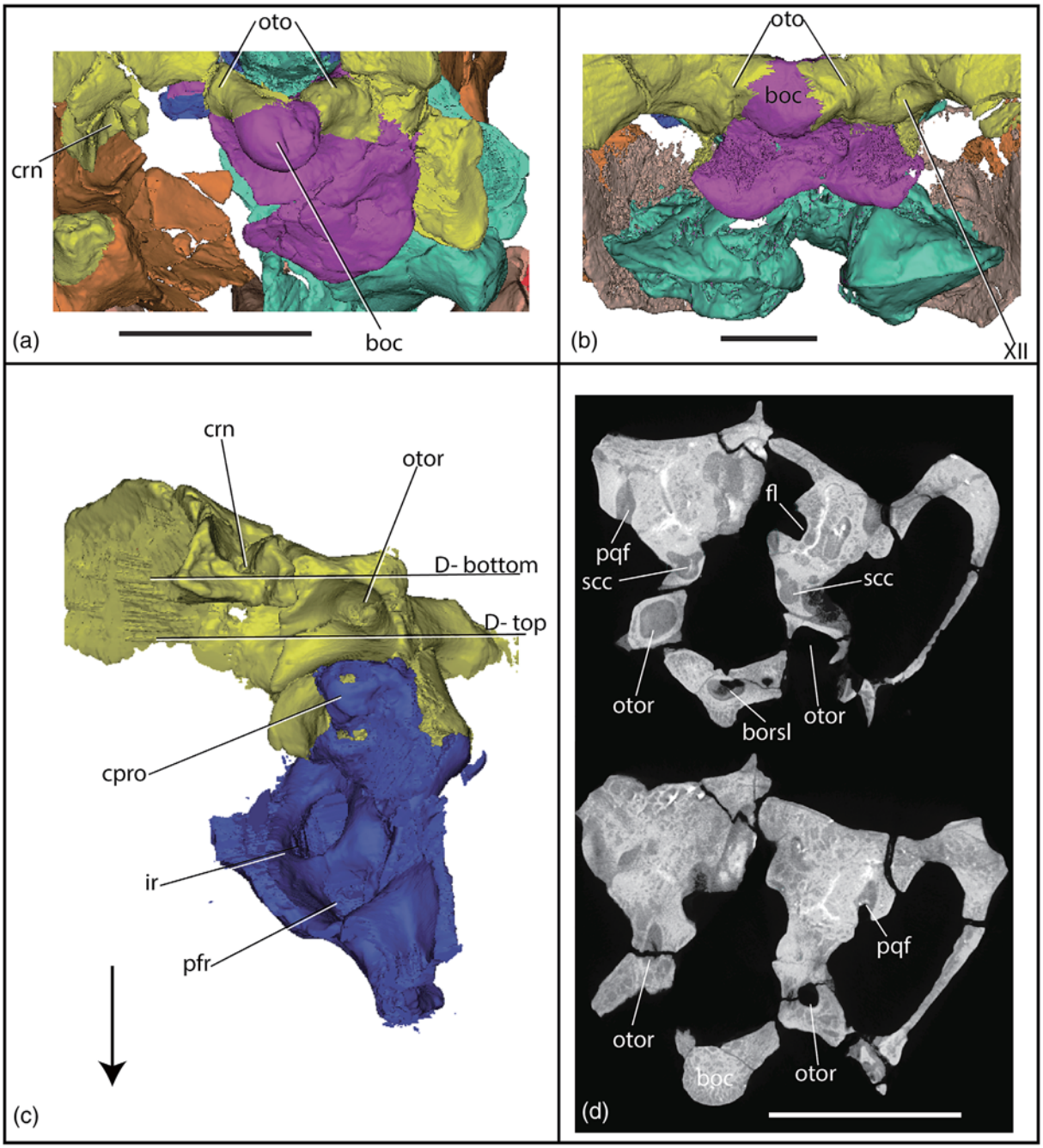

FIGURE 13 Alternative occipital views of CT reconstructions of the skull of (a) *Junggarsuchus sloani* and (b) *Dibothrosuchus elaphros* demonstrating alternative degrees of occipital contribution to the basioccipital condyle; (c) left occipital and prootic of *Junggarsuchus sloani* in ventral view; (d) ventral occipital in anteroposterior CT cross section in *Junggarsuchus sloani* (top slice anterior and bottom slice posterior). Horizontal white lines indicate position of CT slices. Scale bar is equal to 5 mm. Arrow indicates anterior direction.

ventral process of the postorbital overlies the dorsal process of the jugal anteriorly, making up the posterior border of the orbit as in other non-crocodyliform crocodylomorphs, but unlike the unusual condition of *Dibothrosuchus* in which the postorbital is posterior to the jugal and the jugal forms the posterior border of the orbit. However, the condition in *Dibothrosuchus* is similar to the condition seen in crocodyliforms such as *Protosuchus haughtoni* (BP/1/4770) (Gow, 2000), *Orthosuchus* (Nash, 1975), *Fruitachampsa* (Clark, 2011), and extant crocodylians. This descending process in *Junggarsuchus* extends medially as a broad sheet that meets the laterosphenoid (Figure 17c). A descending process along the lateral surface of the laterosphenoid is preserved on the left side, an unusual condition compared to other non-crocodyliform crocodylomorphs. Dorsally, the

suture between the postorbital and the frontal is semicircular in dorsal view, with the convex area directed anteriorly (Figure 9b). The frontal lies medial to the postorbital and the concave posterolateral edge of the frontal articulates with a convex medial edge of the postorbital. A narrow lateral expansion of the frontal borders the postorbital anteriorly. The posterior extent of the postorbital is difficult to determine due to several cracks in the region, and two possible interpretations exist though one would be unusual (Figure 9c,d). The first is that the postorbital has a relatively short posterior process and the squamosal extends far anteriorly. This process is directed posteromedially and is diamond shaped in dorsal view. Its medial edge is bordered by the parietal and potentially a thin portion of the frontal. The lateral edge of the process is sutured to the medial edge of the anterior process of the squamosal. The posterior process of the postorbital reaches the anterolateral edge of the supratemporal fenestra in this interpretation. The contribution to the anterior and lateral edge of the fenestra is short, and three-fourth of the lateral border is made up by the squamosal (Figure 9b).

The more unusual interpretation is that a longitudinal suture between the postorbital and squamosal in the anterior part of the supratemporal bar indicates that the postorbital forms the anterolateral part of the bar and does not border the supratemporal fossa (Figure 9c,d). This interpretation is not clarified by the CT data (broken elements make inferences uncertain), but some of the apparent sutures of the skull roof suggest it. Thus, rather than being medial to the squamosal, as in *Saltoposuchus* and *Dibothrosuchus*, or forming the anterior half of the bar as in *Hesperosuchus* (CM 29894) (Clark et al., 2001), it lies lateral to the squamosal as a long rectangular process, half the length of the squamosal and unlike the postorbital of any known non-crocodyliform crocodylomorph or early diverging crocodyliform like *Protosuchus richardsoni* (AMNH 3024 and UCMP 130860). The posterior extent of the postorbital of this interpretation is unclear, but it apparently ended about half way along the bar. Long posterodorsal processes of postorbital (reaching posterior to the midpoint of the supratemporal fenestra) are known in *Pseudhesperosuchus* (Bonaparte, 1971), *Hesperosuchus* (CM 29894) (Clark et al., 2001), *Sphenosuchus*, and *Almadasuchus* (Pol et al., 2013), but in these taxa, the postorbital is still involved in the lateral border of supratemporal fenestra. A long posterodorsal process has been reported in *Junggarsuchus* by other authors (Leardi et al., 2017) but only in this latter interpretation do we find the processes to be elongated. In the prior interpretation, which is more consistent with Clark, Xu, Forster, and Wang (2004), the posterodorsal process is shorter. The postorbital is strongly concave ventrally where it overhangs the lateral temporal fenestra, continuous with the concavity in the squamosal. In this case, the postorbital is fully excluded from the supratemporal fenestra. This interpretation is supported by the sutures observed on the specimen itself, but neither can be fully supported due to a lack of a clear suture in the CT data and multiple breaks in the region and so have not been scored for either in our matrix.

Only the dorsal portion of the postorbital is preserved in *Dibothrosuchus* (Figures 5 and 10a). The ventral portion of the postorbital bar is preserved on the holotype CUP 2081 (Simmons, 1965). The dorsal portion of the postorbital has a medial ridge that contacts the frontal along a smoothly concave contact. Lateral to this contact, the surface of the dorsal portion of the postorbital is slightly convex and then rises as a concave ridge, unlike the smooth dorsal portion of the postorbital in *Junggarsuchus* (Figure 10c). Both postorbitals are hollow and expanded laterally relative to *Junggarsuchus*, where the postorbitals are narrower and sheet like. The hollow nature of the postorbital in *Dibothrosuchus* is visible due to a posterolateral break in each element, which demonstrates a posterolateral concavity that is floored and roofed by lateral projections of the postorbital (Figure 10b). A broad medial expansion of the postorbital that contacts the laterosphenoid is not found in *Dibothrosuchus*. The postorbital process of the postorbital bar is posterior to the ascending process of the jugal, which is unlike the condition seen in other non-crocodyliform crocodylomorphs, but similar to *Protosuchus richardsoni* (AMNH 3024, MCZ 6727) and other crocodyliforms.

In *Junggarsuchus* the **squamosal** is a kidney-shaped bone in dorsal view that broadly overhangs the infratemporal fossa (Figures 3b, 9b, and 12b). It is broad posteriorly, more similar to *Saltoposuchus* (Sereno & Wild, 1992) than to the narrower squamosal of *Dibothrosuchus* and *Sphenosuchus*. It tapers anteriorly along the lateral edge of the supratemporal fenestra, reaching the anterior edge of the fenestra where it contacts the postorbital laterally. The exact contact between the squamosal and postorbital is unclear, so there are two interpretations of the anterior portion of the squamosal, which have been outlined in the discussion of the postorbital. The first possible condition, which is similar to the conditions seen in non-crocodyliform crocodylomorphs, is a laterally expanded squamosal. In this case, the squamosal still narrows anteriorly, but the postorbital contributes anterolaterally to the supratemporal fenestra and is not excluded from the border by the squamosal (Figure 9b). The anteromedial edge of the squamosal contacts the posterior projection of the postorbital. The alternative interpretation, with a long posterolateral process of the postorbital fully separated from the supratemporal